POR-2229(EX)
(WT-2229)(EX)
EXTRACTED VERSION

OPERATION SUN BEAM, SHOT SMALL BOY

Project Officers Report—Project 6.4

Measurement of Gamma Dose Rate as a Function of Time

S. Kronenberg, Project Officer
B. Markow
I. A. Balton
U. S. Army Electronics Research and Development Laboratory
Fort Monmouth, NJ

11 October 1963

NOTICE:

This is an extract of POR-2229 (WT-2229), Operation SUN BEAM, Shot Small Boy, Project 6.4.

Extracted version prepared for
Director
DEFENSE NUCLEAR AGENCY
Washington, DC 20305-1000

1 September 1985

Destroy this report when it is no longer needed. Do not return to sender.

PLEASE NOTIFY THE DEFENSE NUCLEAR AGENCY, ATTN: STTI, WASHINGTON, DC 20305-1000, IF YOUR ADDRESS IS INCORRECT, IF YOU WISH IT DELETED FROM THE DISTRIBUTION LIST, OR IF THE ADDRESSEE IS NO LONGER EMPLOYED BY YOUR ORGANIZATION.

UNCLASSIFIED
SECURITY CLASSIFICATION OF THIS PAGE

AD-A995376

REPORT DOCUMENTATION PAGE

1a. REPORT SECURITY CLASSIFICATION UNCLASSIFIED	1b. RESTRICTIVE MARKINGS
2a. SECURITY CLASSIFICATION AUTHORITY N/A since Unclassified	3. DISTRIBUTION / AVAILABILITY OF REPORT Approved for public release; distribution is unlimited.
2b. DECLASSIFICATION / DOWNGRADING SCHEDULE N/A since Unclassified	
4. PERFORMING ORGANIZATION REPORT NUMBER(S)	5. MONITORING ORGANIZATION REPORT NUMBER(S) POR-2229 (EX) (WT-2229) (EX)
6a. NAME OF PERFORMING ORGANIZATION U.S. Army Electronics Research Laboratory 6b. OFFICE SYMBOL (If applicable)	7a. NAME OF MONITORING ORGANIZATION Defense Atomic Support Agency
6c. ADDRESS (City, State, and ZIP Code) Fort Monmouth, NJ	7b. ADDRESS (City, State, and ZIP Code) Washington, DC
8a. NAME OF FUNDING / SPONSORING ORGANIZATION 8b. OFFICE SYMBOL (If applicable)	9. PROCUREMENT INSTRUMENT IDENTIFICATION NUMBER
8c. ADDRESS (City, State, and ZIP Code)	10. SOURCE OF FUNDING NUMBERS PROGRAM ELEMENT NO / PROJECT NO. / TASK NO. / WORK UNIT ACCESSION NO

11. TITLE (Include Security Classification)
OPERATION SUN BEAM, SHOT SMALL BOY, Project Officers Report—Project 6.4, Measurement of Gamma Dose Rate as a Function of Time, Extracted Version

12. PERSONAL AUTHOR(S)
Kronenberg, S.; Markow, B. and Balton, I.A.

13a. TYPE OF REPORT	13b. TIME COVERED FROM ____ TO ____	14. DATE OF REPORT (Year, Month, Day)	15. PAGE COUNT
		631011	75

16. SUPPLEMENTARY NOTATION This report has had sensitive military information removed in order to provide an unclassified version for unlimited distribution. The work was performed by the Defense Nuclear Agency in support of the DoD Nuclear Test Personnel Review Program.

17. COSATI CODES		
FIELD	GROUP	SUB-GROUP
18	3	
20	8	

18. SUBJECT TERMS (Continue on reverse if necessary and identify by block number)
Sun Beam; Small Boy; Gamma Radiation; Dosage Rates; Radiation Measurements; SEMIRAD Instrumentation; EMP

19. ABSTRACT (Continue on reverse if necessary and identify by block number)

The primary objective of this project was to obtain measurements of gamma rate as a function of distance and time for evaluation of the electromagnetic (EM) effect. The secondary objective was to measure the gamma rate as a function of distance without involving the EM effect. Such data are of interest in connection with transient radiation effects on electronic components.

A newly developed gamma detector, called SEMIRAD, was used. The reason for choosing this device rather than other conventional gamma detectors is its extremely rapid time response, limited only by the collection time of the secondary electrons, and its high dose-rate saturation limit.

Results of the gamma-dose-rate measurement as a function of time are fragmentary and represent an undistorted measurement in only a few intervals. Failures of equipment and/or

20. DISTRIBUTION / AVAILABILITY OF ABSTRACT	21. ABSTRACT SECURITY CLASSIFICATION	
☒ UNCLASSIFIED/UNLIMITED ☐ SAME AS RPT ☐ DTIC USERS	UNCLASSIFIED	
22a. NAME OF RESPONSIBLE INDIVIDUAL MARK D. FLOHR	22b. TELEPHONE (Include Area Code) 202-325-7559	22c. OFFICE SYMBOL DNA/ISCM

DD FORM 1473, 84 MAR — 83 APR edition may be used until exhausted. All other editions are obsolete.

SECURITY CLASSIFICATION OF THIS PAGE
UNCLASSIFIED

19. ABSTRACT (Continued)

human factors accounted for missing data. The data could be improved in future experiments if changes are made in the instrumentation, i.e., better EM shielding, improved tape recorders and generally higher quality electronics.

FOREWORD

Classified material has been removed in order to make the information available on an unclassified, open publication basis, to any interested parties. The effort to declassify this report has been accomplished specifically to support the Department of Defense Nuclear Test Personnel Review (NTPR) Program. The objective is to facilitate studies of the low levels of radiation received by some individuals during the atmospheric nuclear test program by making as much information as possible available to all interested parties.

The material which has been deleted is either currently classified as Restricted Data or Formerly Restricted Data under the provisions of the Atomic Energy Act of 1954 (as amended), or is National Security Information, or has been determined to be critical military information which could reveal system or equipment vulnerabilities and is, therefore, not appropriate for open publication.

The Defense Nuclear Agency (DNA) believes that though all classified material has been deleted, the report accurately portrays the contents of the original. DNA also believes that the deleted material is of little or no significance to studies into the amounts, or types, of radiation received by any individuals during the atmospheric nuclear test program.

OPERATION SUN BEAM

SHOT SMALL BOY

PROJECT OFFICERS REPORT — PROJECT 6.4

MEASUREMENT OF GAMMA DOSE RATE AS A FUNCTION OF TIME

Stanley Kronenberg, Project Officer

Basil Markow, Deputy Project Officer
I. A. Balton

U.S. Army Electronics Research
and Development Laboratory
Fort Monmouth, New Jersey

ABSTRACT

The objective of Project 6.4 was to measure gamma intensity as a function of time at 625, 1,600, and 4,000 feet using a newly developed gamma detector called SEMIRAD. The gamma intensity was to be measured from several nanoseconds to 90 seconds.

Basically, the SEMIRAD is a vacuum diode. Gamma photons produce Compton electrons in the wall, which, upon leaving the wall, produce low-energy secondary electrons. Without special wall material, such as plastic or fissionable material, the device is almost completely insensitive to neutrons. The reason for choosing this device rather than other conventional gamma detectors is its extremely rapid time response, limited only by the collection time of the secondary electrons, and its high dose-rate saturation limit. The SEMIRAD is saturated only when the secondary electrons are numerous enough to produce space charge big enough to cancel the collecting potential. The signals from this detector were recorded on both the oscilloscopes and magnetic tape. For recording on magnetic tape, the signal was used to pulse a multivibrator whose pulse repetition rate is directly proportional to gamma intensity. The gamma intensity at times later than 10^{-3} to 10^{2} seconds was measured with ion chambers whose output was recorded on magnetic tape using CONRAD instrumentation.

Results of the gamma-dose-rate measurement as a function of time are fragmentary, and represent an undistorted measurement in only a few intervals. Failures of equipment and/or human factors accounted for missing data. The data could be improved in a future experiment if specific changes are made in the instrumentation, viz: better EM shielding, improved tape recorders, and generally higher quality electronics.

PREFACE

The following USAELRDL personnel contributed to the design, performance, and data analysis of this experiment and to the preparation of the report: Michael Basso, Alice Bogart, James Brown, George Bryan, Vernon Bryan, Frances Calafato, Gilbert Cantor, Charles Coates, Joseph Crotchfelt, George Fegan, Eric Ellstrom, Mildred Forsythe, William Gallas, Charles Ganers, Joseph Giacalone, Caroline Grossman, Gerald Healey, Bud Housfield, Ockle Johnson, Frank Kowalczyk, Ross Larrick, John D. Lloyd, William Lonnie, James McMahon, Edward Mooney, Vernice Morris, Kristian Nilson, Charles Olsen, Charles Pullen, Richard Rast, Lillian Sacher, Albert Schwartz, John Schwartz, Loretta Schaad, Linda Solcum, Robert Steinek, Lillian Steelman, and Harry Van Gorden.

CONTENTS

TABLES

FIGURES

CHAPTER 1

INTRODUCTION

1.1 OBJECTIVES

The objective of Project 6.4, Operation Sun Beam, was to obtain measurements of gamma rate as a function of distance and time for evaluation of the electromagnetic (EM) effect. These measurements were made at distances of 625, 1,600,and 4,000 feet from ground zero and for the following times: 0 to 0.1 μsec; 0 to 10 μsec; 0 to 1 msec; and 1 msec to 100 seconds. Figure 1.1 shows the layout of the stations.

The gamma rate as a function of time was measured at Station I (625 feet) for the 4π geometry and for the gammas coming directly from the device (collimated measurement).

The secondary objective was to measure the gamma rate as a function of distance as outlined above without involving the EM effect. Such data are of interest in connection with many problems: e.g., transient radiation effects on electronic components. Knowledge of the gamma environment would also be helpful in the construction of laboratory devices that simulate radiation delivered from atomic devices.

1.2 BACKGROUND

The primary purpose of Project 6.4 was to obtain data necessary for the theoretical explanation and evaluation of the EM effect. This effect has been neglected in previous experiments, but its study is of interest because of the impact it may have on the battlefield

environment and especially on electronic components in friendly or enemy instrumentation. Measurements obtained by Project 6.4, together with those obtained by other projects in Programs 6 and 2, Operation Sun Beam, are expected to provide the necessary data.

Measurements of the gamma rate as a function of distance and time were never before measured for some of the times and distances outlined in Section 1.1. In the past, measurements covered the alpha rise of the radiation very close to the device and the gamma rate as a function of distance and time at about 1,500-foot distances for times later than 1 msec. The latter measurement, which was made on Operation Plumbbob (Reference 1) and repeated on Project 6.4, is described in Chapter 2.

A number of reasons are offered for the lack of gamma-rate information for times between 0.1 usec and 1 msec. First, in parts of this time interval, the EM effect is very strong and influences the sensors so that the readout instrumentation is inoperative. Thus, very elaborate EM shielding is necessary to obtain valid data. Second, within this time interval, fast neutrons from the fission reaction arrive at distances between several hundred and several thousand feet from ground zero and affect the ion chamber as well as the phosphor-plus-light instrumentation. At some distances and times, the fast-neutron rate may be much higher than the gamma rate, and thus the gamma data may be very doubtful. Therefore, for valid gamma measurements, the fast-neutron rate and the fast-neutron spectrum as a function

of time should be known at the point of the gamma measurement, and the gamma sensors should be strongly insensitive to fast neutrons. Both of these conditions were to be satisfied in Project 6.4. Third, the dose rate changes very rapidly during the critical time interval. Therefore, wide-sensitivity-range instrumentation with high time resolution was necessary, and this instrumentation was to be designed so as not to saturate at very high radiation levels. In addition, the radiation sensors that measure the dose rate as a function of time were not to be damaged by the total dose. Such damage affects the sensitivity of the device, and the results become unreliable. This shortcoming applies especially to scintillation phosphors. An electron traversing a phosphor produces a track about 10^{-8} cm in diameter and about 1 cm in length. Thus, a volume of about 10^{-16} cm^3 is created where the temperature reaches several thousand degrees (without reaching thermal equilibrium). This condition results in destruction of the affected volume; and after 10^{16} electrons hit the phosphor, virtually no phosphor is left. Long before such damage takes place, the phosphor starts to change its sensitivity. Another effect was observed with scintillating phosphors in Godiva II experiments wherein apparently some afterglow took place immediately following a high-intensity exposure (Figure 1.2). Phosphors give excellent results for a rising radiation intensity, but when the intensity reaches a peak and starts to decline, results obtained with a phosphor-light detector system are doubtful. Therefore, this type of detector

was not used in Project 6.4. For the measurement of gamma rates in accordance with Project 6.4 specifications, the best possible system was the SEMIRAD (secondary-electron mixed-radiation dosimetry). SEMIRADS can be built so as to be sensitive to gammas only or to neutrons only. Project 6.4 used the gamma-diode-type SEMIRAD.

1.3 THEORY

1.3.1 Description of SEMIRADS. SEMIRADS have the same general appearance as do ion chambers; however, unlike ion chambers, SEMIRADS are evacuated to a very low pressure. As a consequence, little or no ionization is produced in SEMIRADS, and the entire response is due to secondary electrons.

When the wall of a SEMIRAD is irradiated with X-rays or gamma rays, a number of particles are ejected. These particles are photoelectrons and Compton electrons. For gamma energies above 2 Mev, these particles include both positrons and electrons from pair production. When these electrons pass through the surface of the wall of the SEMIRAD chamber, they cause secondary-electron emission. Secondary electrons are also emitted when the high-energy Compton and photoelectrons or protons reenter the opposite wall of the chamber (Figure 1.3). If a positively charged electrode with an applied voltage higher than the energy of the secondary electrons is placed within the chamber, the secondary electrons are swept up, and the total charge collected is proportional to the radiation dose received.

Since the energy of most of the secondary electrons is not very high (below 50 ev), only a moderate voltage need be applied

to ensure complete collection. The primary particles are not collected because their energy (in the Mev range) is much too high to be affected by the collecting potential.

Since SEMIRAD operation depends not on the collection of relatively heavy positive and negative gas ions but on the collection of electrons alone, recombination effects do not occur. Thus, SEMIRADS do not saturate at high dose rates. Furthermore, because of the rapid collection of the secondary electrons (owing to the small inertia of electrons as compared with ions), the response time of SEMIRADS is approximately one millionth that of conventional ion-chamber dosimeters. In general, the time necessary to collect electrons in a two-electrode system is given by the nonrelativistic expression:

$$t = (2d^2m/ev)^{\frac{1}{2}} \qquad (1.1)$$

Where: d = distance between the electrodes

m = electron mass

v = applied voltage

e = charge of the electron

In practical applications, these times are much shorter than the time resolution of the electronic equipment necessary to amplify and record the increased pulse. Thus, the latter sets the actual limit for the time resolution.

1.3.2 Shielding Against EM Effect. The EM effect from the device is very strong during the early times of the measurement. Therefore, the influence of the EM effect on the gamma measurement

must be eliminated. Every sensor above ground and every piece of recording equipment in the bunkers is a potential antenna that may pick up the EM signal. These instruments must, therefore, have tight electromagnetic shielding.

According to theory, a perfect electromagnetic shield can be obtained by surrounding the volume to be shielded with a vacuum-tight cover made of a perfect conductor. The thickness of the shield is not important. In practice, the shielding has to be thick and of a material with high conductivity and preferably high permeability. For the bunker construction, welded 1-inch soft-steel plates were used for lining the inside of the concrete wall. The dome containing the radiation sensors was made of ½-inch-steel plates, and the pipe through which the coaxial cables were fed from the detectors to the recorders was made of heavy wall steel. Special precautions had to be met to avoid EM leaking through the manhole and through the hard-wire connection that activated the cameras in the bunker from the control point. These precautions were accomplished by the use of metallic packing on the points where the manhole and its cover met.

The cable that provided the signal to open the cameras was loaded with explosive and was destroyed immediately after transmission of the signal to the cameras at minus 2 seconds. A spring-loaded plate then closed the small opening through which the cable entered the bunker. The system was then completely separated by steel from the outside world. A battery-driven timing switch opened all circuits at plus 2 minutes.

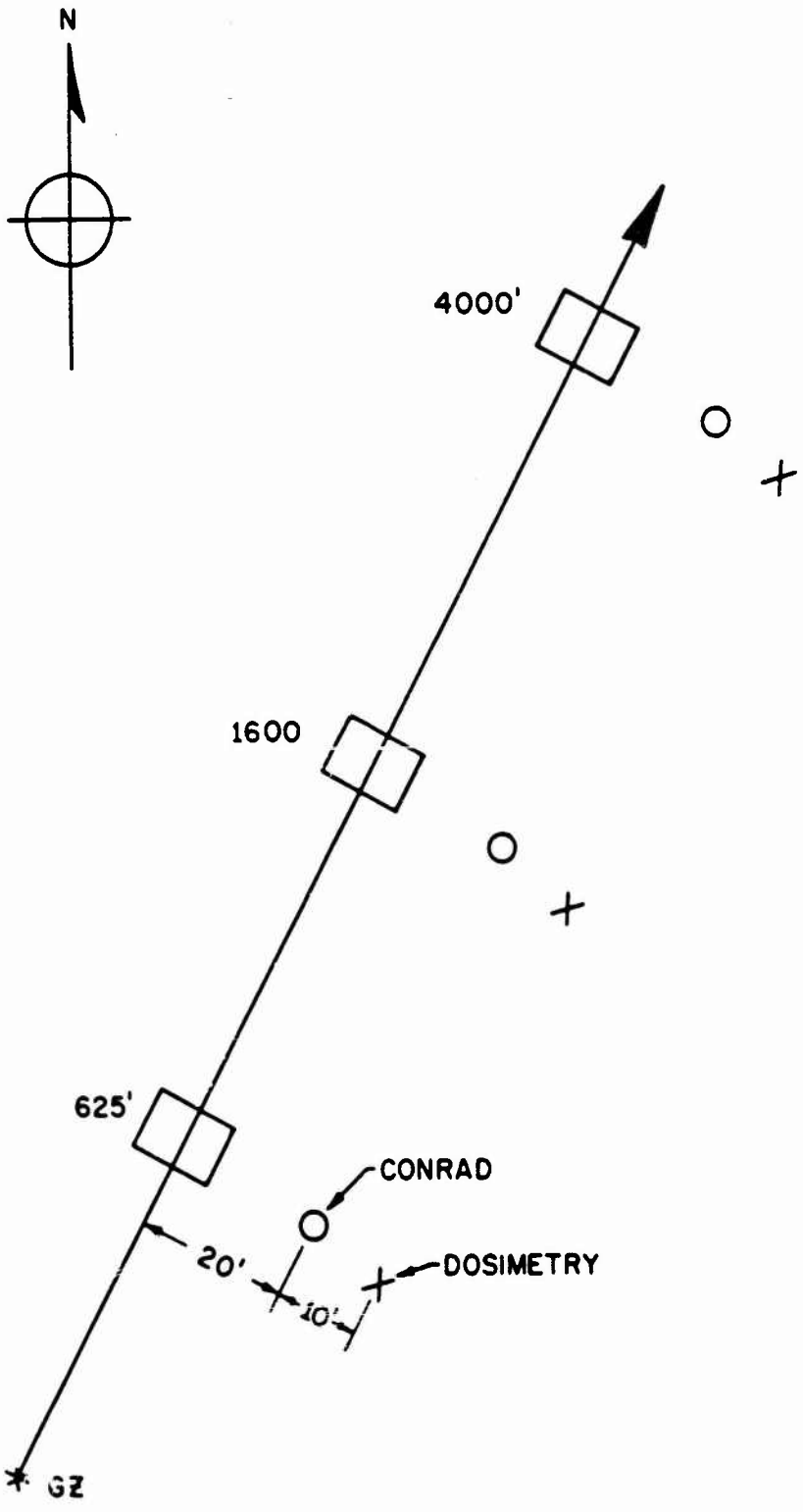

Figure 1.1 Station layout.

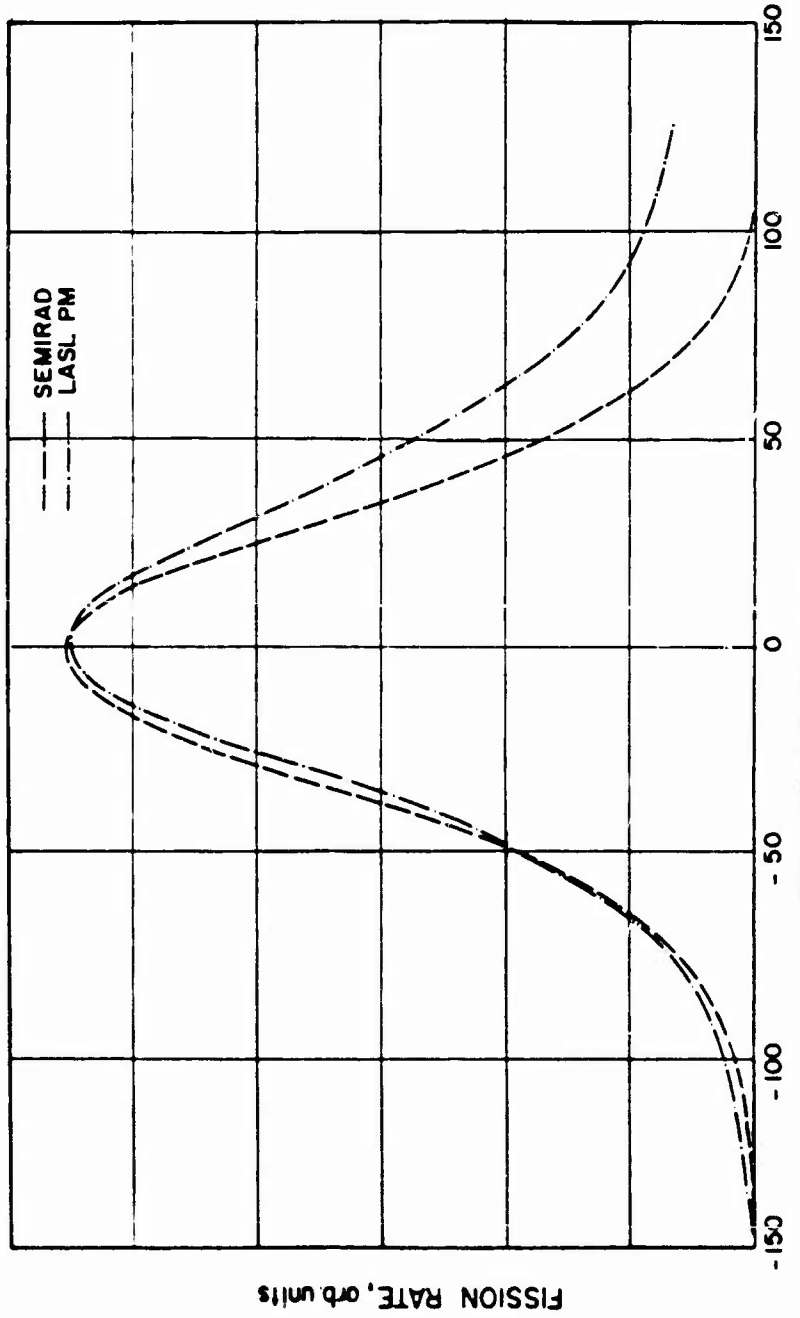

Figure 1.2 Godiva II pulse recorded by a photophor phototube and by a SEMIRAD diode.

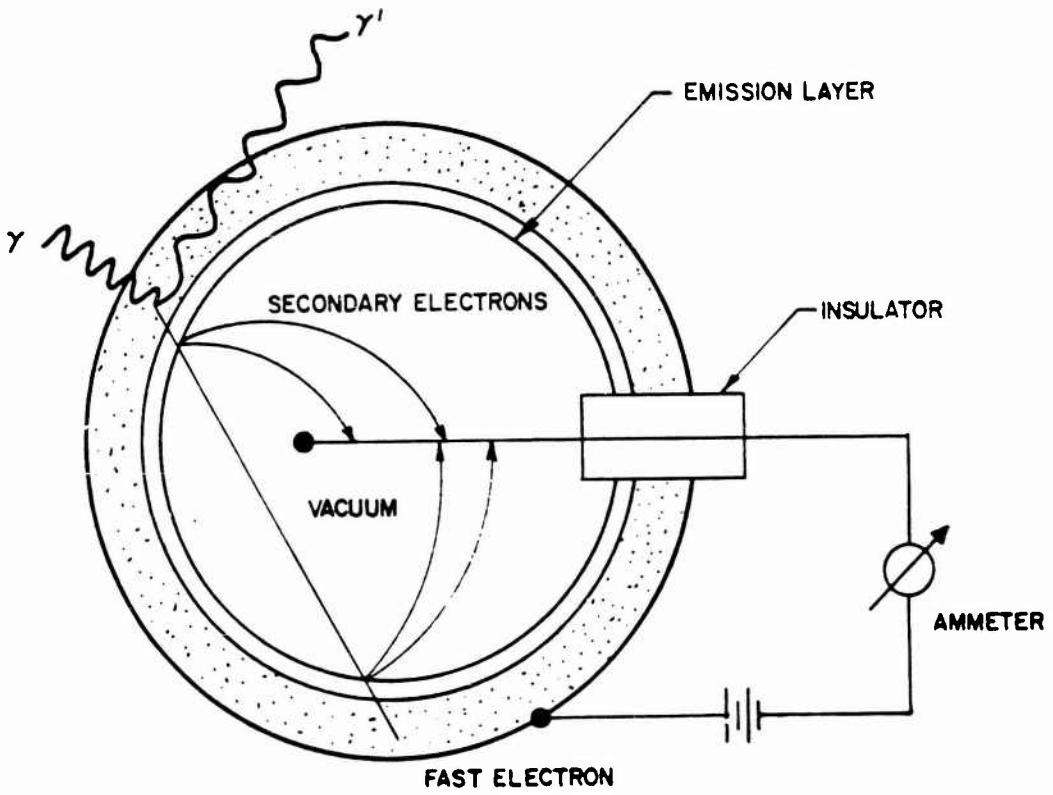

Figure 1.3 Principle of the gamma SEMIRAD diode.

CHAPTER 2

PROCEDURE

2.1 OPERATIONS

2.1.1 Shot Participation.

The device had to be fired 10 feet above the ground in order to make one collimated gamma measurement possible at the 625-foot station. The device was to be symmetric with respect to the vertical axis to make the measurement on the ground as independent as possible of direction.

2.1.2 Test-Site Activities. All instrumentation was assembled and tested in the quonset area at the Nevada Test Site (NTS). Gamma detectors were calibrated on a 100-curie Co^{60} source. The oscilloscopes were installed in the bunkers and the associated detector simulators positioned in their blast shield prior to the start of the preshot dry runs. Auxiliary equipment, as required, was used to check out systems and timing signals during the dry-run tests. Oscilloscope power supplies were checked during the dry runs.

The detector-tape systems (CONRADS) were installed in each bunker. These systems were powered by dry cells. The auxiliary stations (outside stations) were entirely self-contained.

After completion of dry runs, the real sensors replaced the simulators, and final adjustments were made on oscilloscopes and cameras. Tape-recorder systems were loaded and secured. Power units were serviced and started as late as possible prior to evacuation.

A camera record was made of each zero-amplitude sweep under the latest possible preshot conditions to record the baselines on the scopes. A complete documentary photo of each equipment setting was required just prior to evacuation. After the inside of the bunker had been secured, the access plug was inserted and sealed, using heavy cranes to lift the concrete plugs. This late evacuation also applied to Project 2.2.

All stations were activated by hard-wire timing signals furnished by Edgerton, Germeshausen, & Grier, Inc. (EG&G). Timing-signal wires entering a bunker were destroyed just after the signal activated an appropriate relay, in order to eliminate an effective antenna leading an EM pulse into the bunker. This requirement did not apply to the auxiliary stations.

Personnel-range gamma dosimetry was required inside the bunkers. Wide-range dosimetry was required inside each blast shield, and a double set of gamma dosimetry (one for rapid recovery and one to await station recovery) was placed outside. Total-dose gamma-dosimetry requirements were coordinated with the project responsible for gamma dosimetry: Nuclear Defense Laboratory (NDL), Edgewood Arsenal, Maryland. A complete set of neutron-foil measurements was required at or near the blast shield of each bunker. In addition, gold and sulfur measurements were required inside and outside every blast shield and inside the connecting pipes. The neutron-measurement requirements were coordinated with responsible NDL personnel. The gamma-and-neutron dosimetry requirements also applied to Project 2.2.

Reentry was accomplished when Rad-Safe conditions permitted. When reentry was accomplished, the stations were opened by a specially trained and prepared crew. A USAELRDL crew entered the bunkers, photographed instruments, removed plate holders from cameras, placed these holders in a lead box for fog protection, and left the bunker.

Reentry was a joint effort between Projects 6.4 and 2.2. Equipment and instruments of both projects were removed at a later date determined by radiation levels existing at each bunker.

2.2 INSTRUMENTATION

2.2.1 SEMIRAD Techniques and Theory. The appendix describes the SEMIRAD instrumentation and includes a discussion of sensitivity, vacuum considerations, dose-rate limitations, and energy dependence.

2.2.2 Gamma Diodes. The gamma diodes used by Project 6.4 were manufactured by Eon Corporation, Brooklyn, New York, according to USAELRDL design (Eon Type 7316). Figure 2.1 is an engineering drawing of the gamma diode. For use in a high-intensity field, the instruments must be placed in a housing, and every component must be potted with an insulating material to prevent ionization effects. Figures 2.2a and 2.2b are photographs of a finished sensor. The wall material and the collector were titanium. The insulator between the electrodes was alumina and was vacuum-soldered to the titanium with nickel. The evacuation tube was soft copper. All parts of the diode were outgassed at 500° C before the evacuation, and a vacuum of about

10^{-6} mm Hg could thus be obtained. This vacuum was important for reproducibility of tube sensitivity: in fact the measured sensitivity varied by only a few percent among the individual sensors, provided that the vacuum was maintained. Several diodes had apparently developed cracks in the ceramic when exposed to moderately rough handling and had partially lost their vacuum. Faulty instruments were replaced by spares.

2.2.3 Calibration of SEMIRAD. SEMIRAD dose-rate meters produce an electric current, which is converted into rads/hr. There are two methods of conversion: (a) calibrate the sensitivity at constant low-radiation rates and thus obtain the absolute sensitivity of the instrument in amp/r/hr; and (b) calibrate for sensitivity during the measurement of a high-intensity pulse.

Calibration at low intensities. SEMIRAD diodes are very insensitive devices; thus, at several hundred to several thousand rad /hr, as delivered from a typical laboratory X-ray machine or radioactive source, the output is very small. Therefore, sensitive current-detection methods have to be used. The collector electrode is connected with a shielded cable to the input of a Keithley 610A electrometer (or equivalent) outside of the radiation area. In this way, currents of 10^{-12} amperes can be read. The absolute sensitivity is obtained by dividing the output current by the constant dose rate. On the Project 6.4 diodes, an average sensitivity of

2×10^{-15} amp/r/hr was obtained for Cs^{137} gammas. This data was for perpendicular incidence of the radiation to the axis of the instrument. When the X-rays were shot at the SEMIRAD from the high-voltage connector side through the high-voltage connector (parallel to the axis of the instrument), the resulting sensitivity was 9×10^{-16} amp/r/hr. The instruments were also calibrated on a 750-kv X-ray machine at 6,500 r/hr (filtered with 1.1-mm Cd). The above sensitivity values were not reproducible even for one and the same instrument. The neutron insensitivity was less than 0.1 percent and was established earlier in experiments on the Van de Graaff generator and on the Sandia Pulsed Radiation Facility (SPRF).

Calibration during exposure to a high-intensity pulse. Assume $I = I(t)$ is the measured current from the SEMIRAD as a function of time for a given radiation pulse measured with the SEMIRAD. Then $\int_0^\infty I(t)\,dt = Q$, where Q is the total charge of secondary electrons delivered from the instrument during the pulse. According to the principle of operation of the SEMIRAD, $Q = KD$, where D is the total dose of radiation delivered during the pulse. The term D can be measured by use of an independent method for measuring total radiation doses delivered at high rates (for example, film dosimeters for gamma rays). The total charge, Q, is obtained from graphical or numerical integration of the curve I(t), and thus the proportionality factor K can be determined. Differentiating the above expression

gives the expression for current as a function of dose rate:

$$I(t) = dQ/dt = K\ dD/dt = KD_r(t) \qquad (2.1)$$

Equation 2.1 is the conversion from current reading to dose rate in rads per hour and can be used to calibrate the SEMIRAD during the pulse reading. The instruments were calibrated and checked using the above methods at the SPRF and at the LINAC (White Sands Missile Range). At the LINAC, the instrument was bombarded directly with 8-Mev electrons in a 9-μsec pulse to check its behavior at rapidly changing high dose rates (Figure 2.3). For comparison, the light output from a phosphor was recorded under similar conditions but at much lower dose rates (Figure 2.4). Note that the behavior at the beginning of the pulse is similar for both the SEMIRAD and phosphor systems, but at the end of the pulse, the SEMIRAD shows a faster response. Figure 2.5 shows the gamma pulse obtained at the SPRF. The time scale was 50 μsec per division. From the known total dose at the point of measurement, we obtain $2.52 \cdot 10^{-16}$ amp/r/hr as the sensitivity for fission gammas. This figure is lower by one order of magnitude than the sensitivity measured at the dc low-intensity calibration. This lower value is reproducible and varies by only a few percent among the individual instruments, if the vacuum in the diode is high and unchanging. It is the only usable value, because the low-intensity calibration is affected by cable effects and other

side effects; at high intensity, these effects are strongly saturated and do not contribute to the signal.

2.2.4 Condenser Bank and Battery Power Supply. To keep the voltage on the wall of the instrument constant during a fast surge of current, a condenser bank was inserted between the high-voltage part of the instrument and ground. This bank consisted of ten 10^3-μμf low-inductance capacitors fed through a 150-ohm resistor. To protect the capacitor bank from radiation effects that might superimpose unwanted signals upon the rate-versus-time trace, the condensers were placed inside the cable pipe that connected the bunkers with the detector housing (for short readout times), and inside the bunkers (for long readout times). Figure 2.6 shows the disassembled condenser bank.

2.2.5 Collimated Measurement. At the 625-foot station, a collimated gamma measurement was made to determine the difference between the direct and the direct-plus-scattered gamma flux. Since the firing of the device was scheduled to take place only 10 feet above ground, a very careful collimator design was necessary to avoid radiation scattered from the ground. A three-plate collimator was designed for this purpose. The first plate prevented the nondirect radiation from reaching the instruments. The third plate cut off the gamma rays scattered at the edge of the openings in the first and second plate. Figure 2.7 is a schematic view of the collimator. To

satisfy the necessary conditions, the following relations must apply:

$$\frac{h}{D - l/2} = \frac{d/2}{l/2} \quad , \quad \frac{m/2 - d/2}{l/2} = \frac{h + d/2}{D - l}$$

and

$$\frac{l/2}{m/2 - d/2} = \frac{l/2}{s/2 - m/2}$$

or $$l = 2D\ d/2h + d$$

$$m = \frac{2hl + dl}{2\ (D-l)} + d$$

$$s = 2m - d$$

The meaning of the symbols is evident from the Figure 2.7. By choosing d = 4 cm, which comfortably covers the diameter of the sensors, and substituting h = 260 cm and D = 189 m, the following edge values of the collimator openings are obtained: m = 4.09 cm, s = 4.18 cm, and l = 291 cm. To make sure the second and third plates were in the shadow in respect to the direct radiation, m = 4.5 cm and s = 5 cm were chosen for the design. Two sensors (gamma SEMIRADS) were placed side by side behind the last plate. Figure 2.8 shows the assembly and the cable layout for the collimated gamma measurement. Short times only were of interest here, and therefore readout on oscilloscopes only was used for this measurement.

2.3 DATA REQUIREMENTS

2.3.1 Data Required and Predicted Reliability. Figures 2.9, 2.10, and 2.11 show the expected gamma dose rate as a function of time for the three stations. The figures were computed by use of data contained in Reference 3.

2.3.2 Method of Recording Data. The early times (up to 1 msec) were read by use of banks of oscilloscopes. Connection between the sensors and the readout oscilloscopes was accomplished with coaxial cables. The cables were 1/2-inch Foamflex with solid dielectric to avoid ionization effects in the cables. The cable impedance was 125 ohms to match the Tektronix-519 scope (used for early time recording). The rise time of the pulse in the cable was less than 2×10^{-9} seconds. The other scopes used for recording were Tektronix 555 and 551. Both have an input impedance of 1 megohm, and therefore the 125-ohm terminating resistor can be applied here, too. The cables were terminated at the scope. Figures 2.12, 2.13, and 2.14 are schematics of the recording system in Bunkers E, F, and G. Time scales and sensitivity settings are given with each scope trace. To make possible corrections for EM effects, radiation effects in the cables, and other unpredictable effectsto the signal, we used two dummy SEMIRADS at each station, without a central electrode (to avoid primary electron contribution), and with potting compound in place of the vacuum; otherwise, they were constructed in the same way as the other gamma diodes.

Their signals (if any) were recorded on a separate bank of oscilloscopes.

For the evaluation of the oscilloscope photos, it was important to know the total dose for gammas delivered only by the initial radiation up to approximately 60 seconds. To obtain this measurement, 5-inch-diameter aluminum pipes were buried 10 feet deep in the Nevada soil at points close to the bunkers where the measurement was desired. A blast switch released a dosimetry package that dropped to the bottom of the pipe where the total fallout dose was low. During the recovery procedures, the package was collected for evaluation (Figure 2.15). To observe the environment other than radiation in the vicinity of the instruments, temperature and shock were recorded as functions of time. These data were taken to make possible corrections on the gamma-rate recordings should the necessity arise.

To measure the gamma fluxes as a function of time at times later than 1 msec and up to 100 sec, a modified CONRAD instrumentation (Reference 1) was used. CONRAD sensors are ionization chambers. The readout system is self-contained, battery-powered, and uses tape recorders. Some questions exist concerning the reaction of CONRAD to the fast neutrons that are present together with the gamma rays, and concerning the contribution of gamma rays produced by neutrons in the blast shield and the instrument housing. To answer these

questions, CONRAD devices were used together with gamma SEMIRAD and triode SEMIRAD systems (Reference 7). The rough signal from these sensors was processed as in the case of the ionization chambers and was recorded on the three free channels of the tape recorder.

Two CONRAD systems were mounted at each station: one a self-contained system in a pit next to the bunker, and one with the detectors next to the other detectors in the instrument shield (which was an integral part of the bunker with the tape readout in the bunkers). In addition, Station F had a third outside CONRAD station shielded with iron. Figures 2.12, 2.13, and 2.14 include diagrams of the aluminum-shielded CONRAD stations next to Bunkers E, F, and G, and of the steel-shielded station at Bunker F.

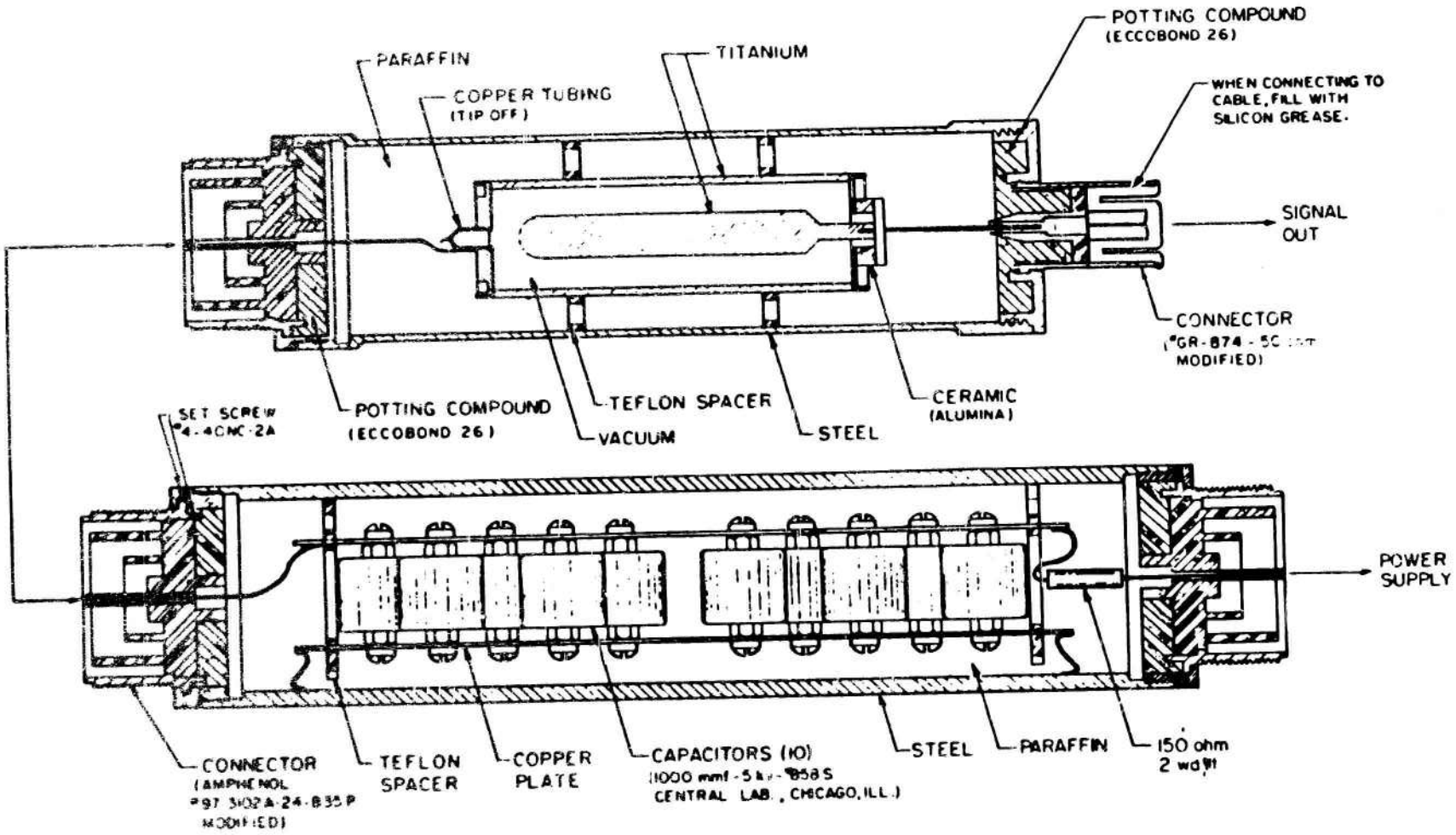

Figure 2.1 Construction of a SEMIRAD diode and its condenser bank.

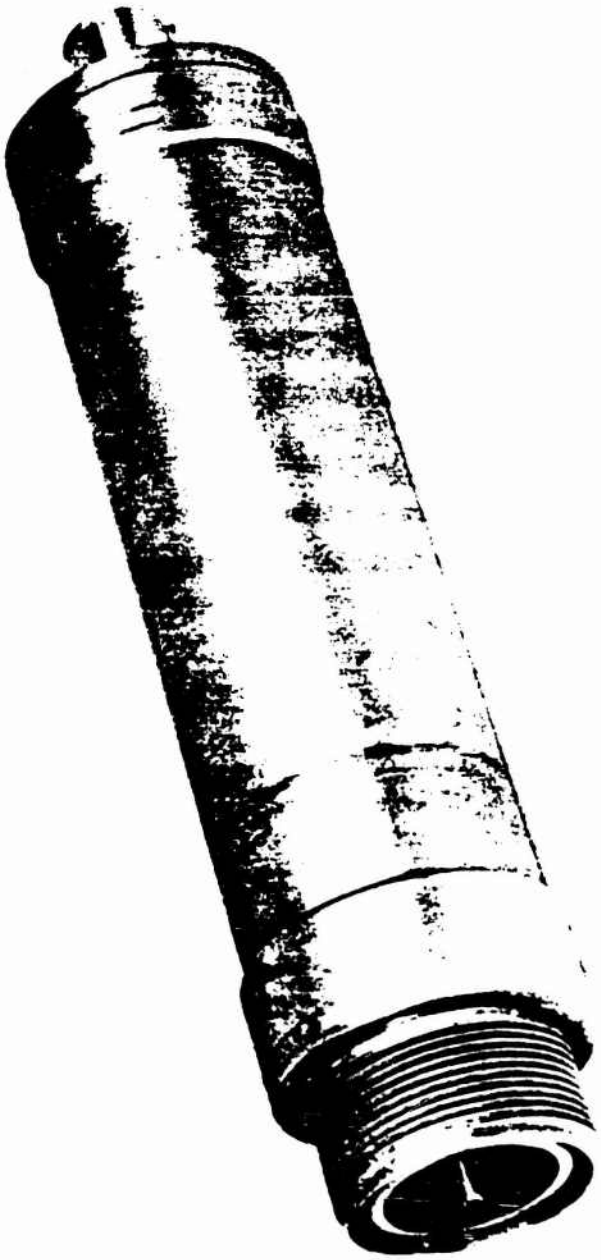

Figure 2.2a Assembled SEMIRAD diode system. (SIGRA/SL-62-586)

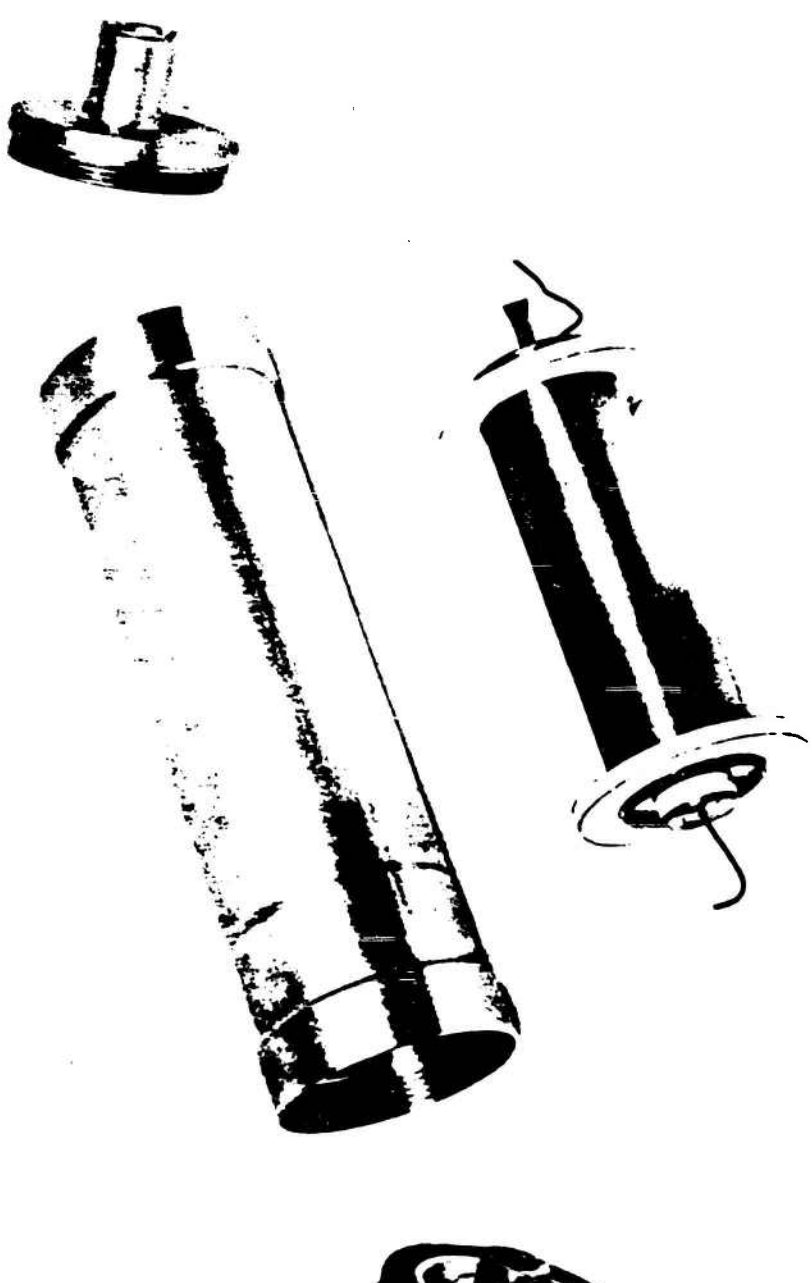

Figure 2 2b Components of the SEMIRAD diode system. (SIGRA/SL-62-587)

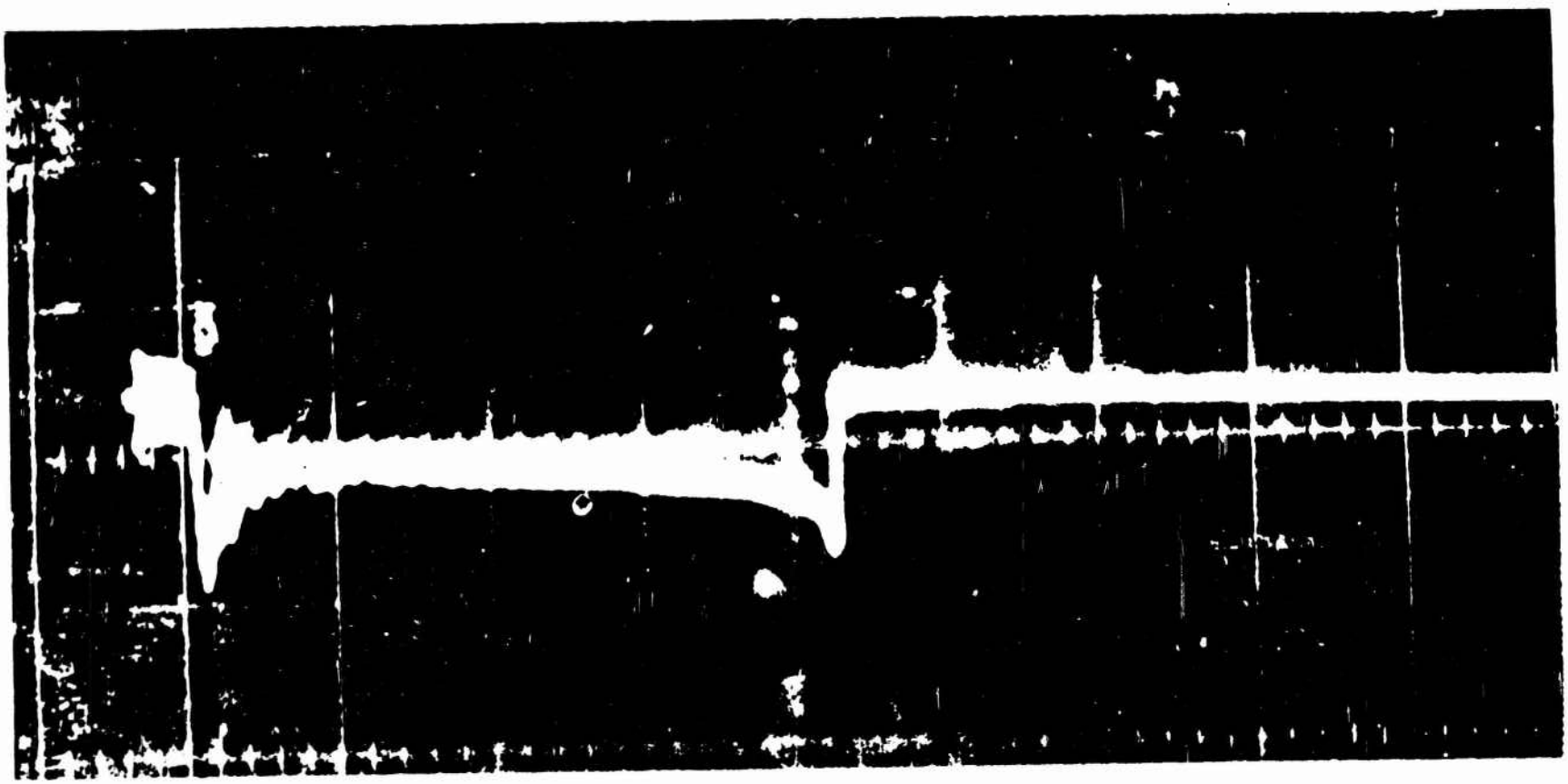

Figure 2.3 White Sands Missile Range LINAC pulse, recorded with the SEMIRAD diode system. (FCNTS 62/1105D)

Figure 2.4 Same pulse as in Figure 2.3. recorded with a phosphor-photo detector system.

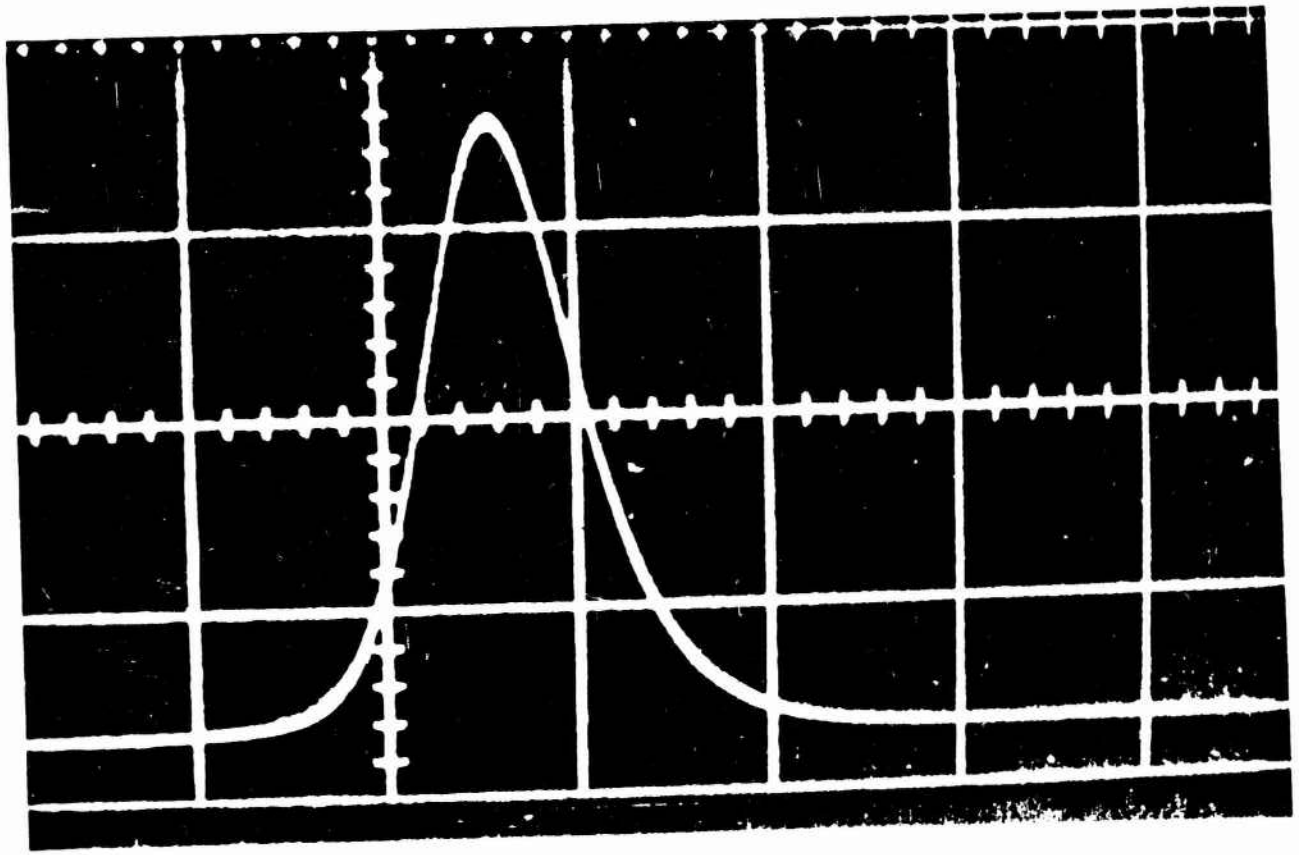

Figure 2.5 SPRF pulse, recorded with a SEMIRAD diode (sweep: 50 μsec/cm).

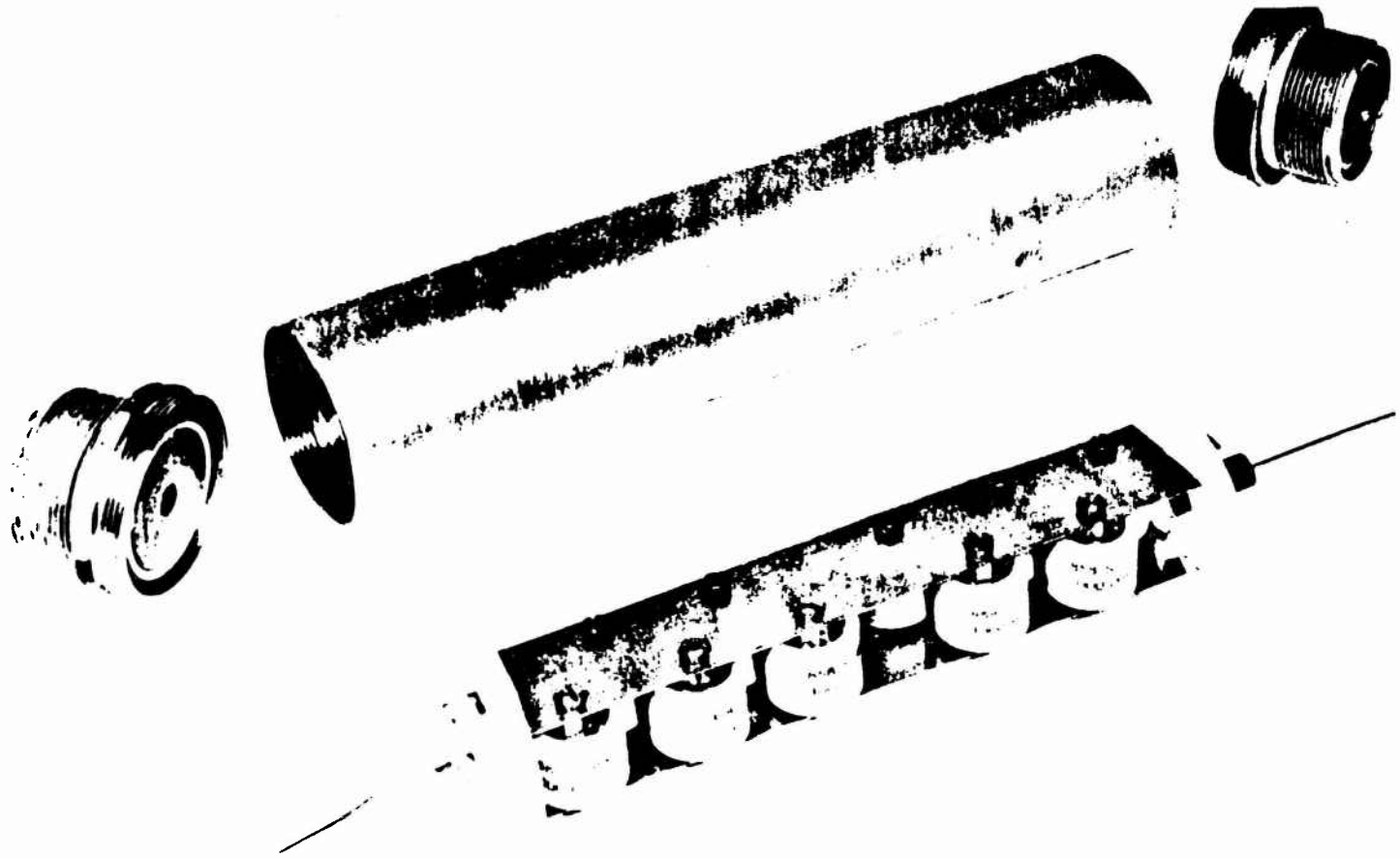

Figure 2.6 Components of a condenser bank used in conjunction with the SEMIRAD diode. (SIGRA/SL-62-585)

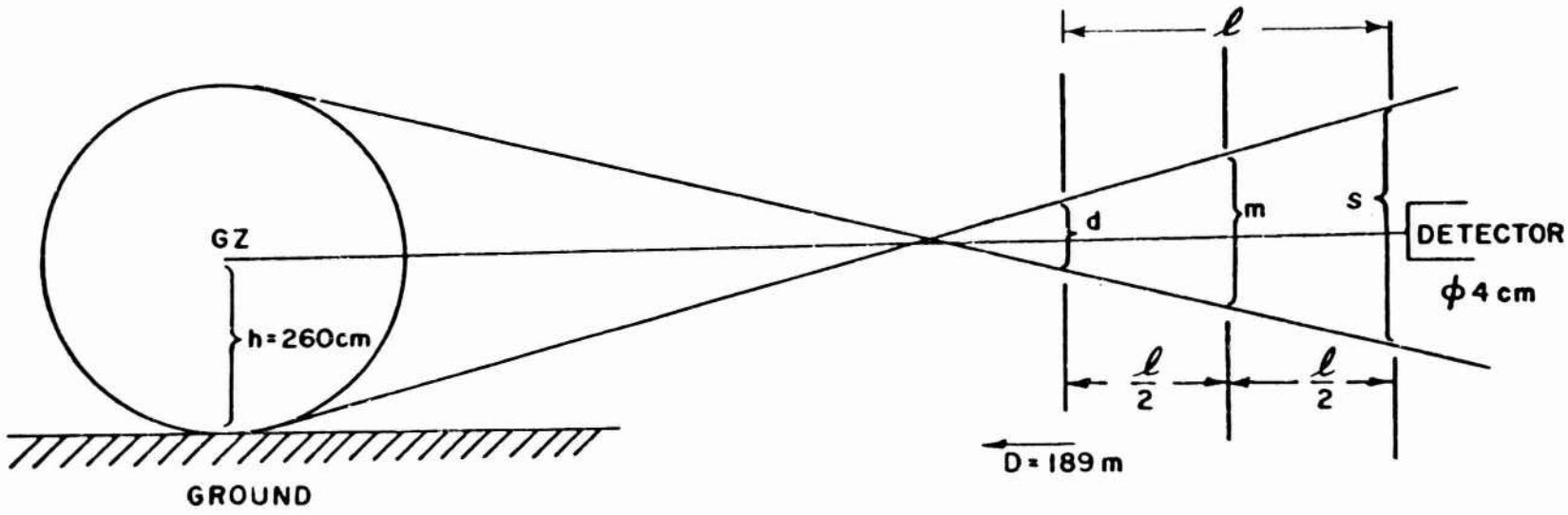

Figure 2.7 Schematic diagram of the collimator.

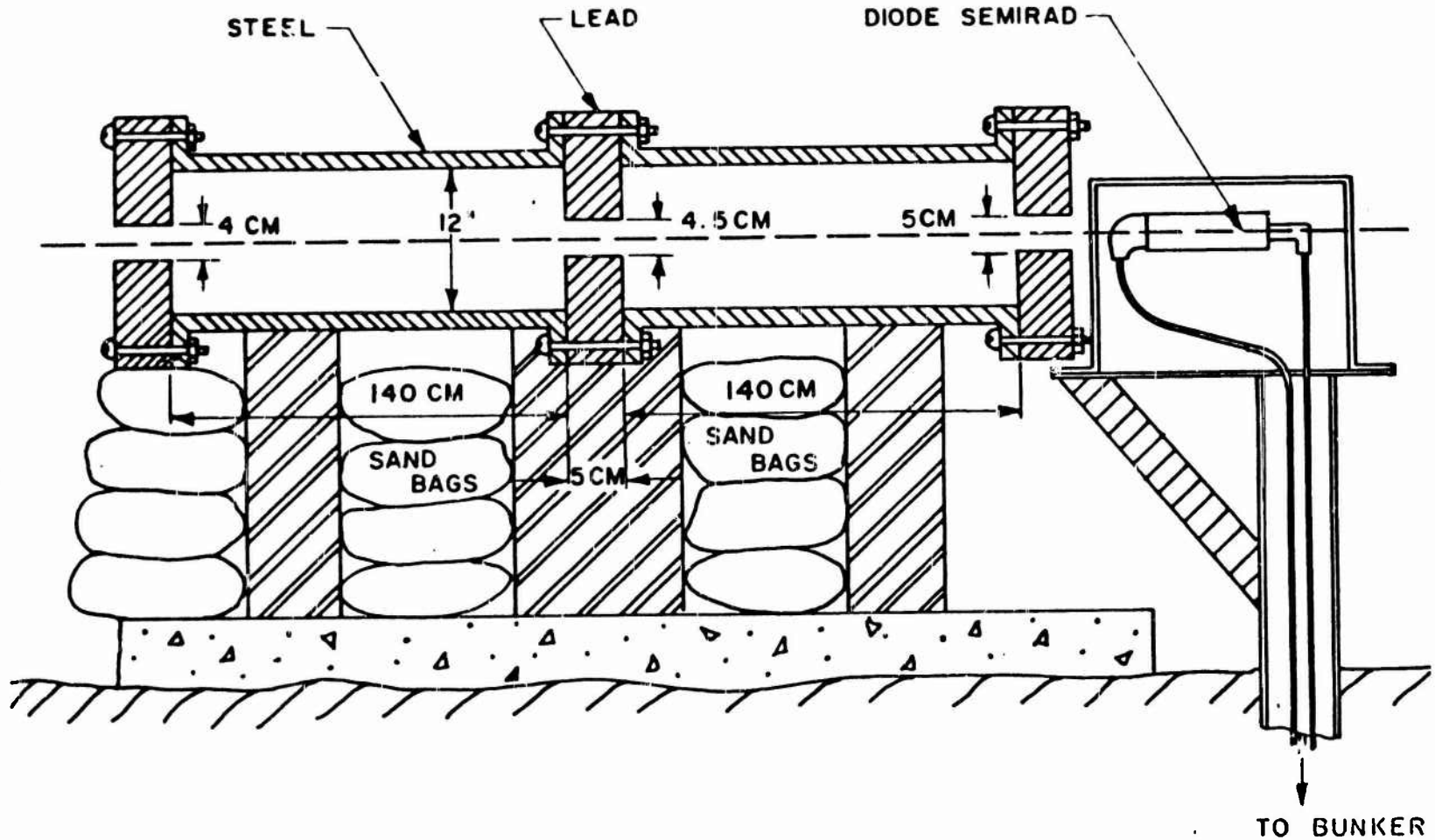

Figure 2-8 Collimator assembly and installation.

Pages 42 through 44 deleted.

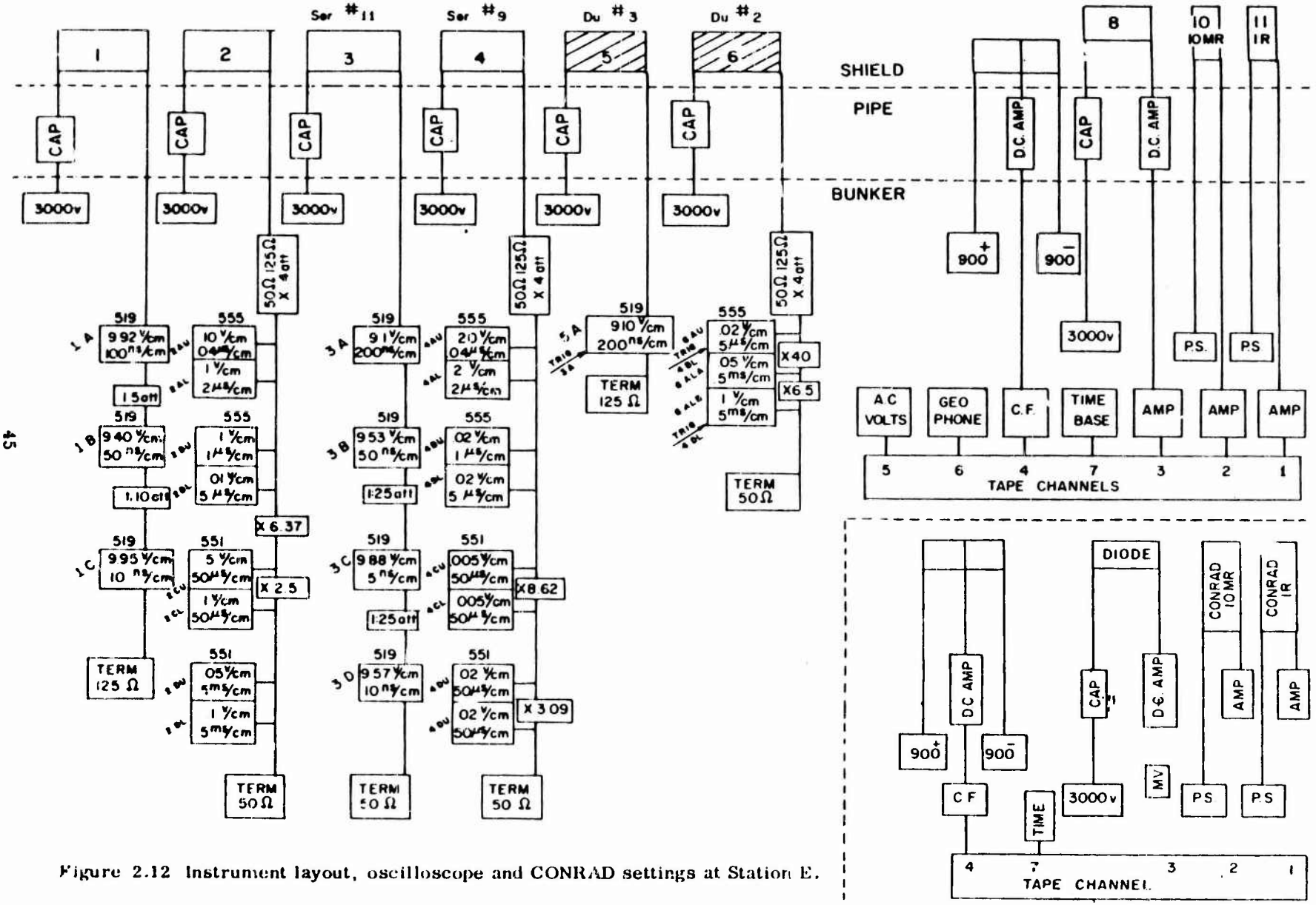

Figure 2.12 Instrument layout, oscilloscope and CONRAD settings at Station E.

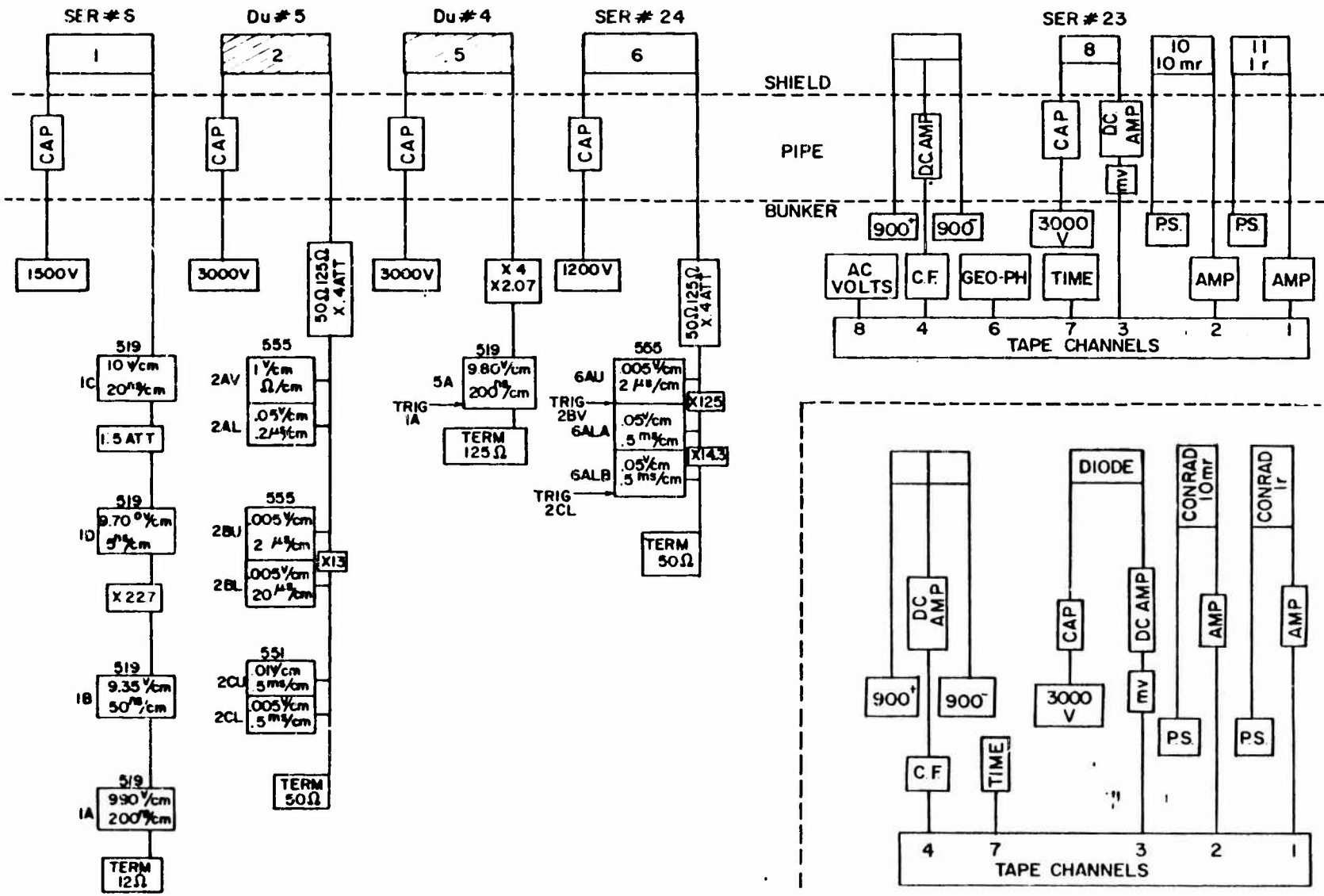

Figure 2.13 Instrument layout, oscilloscope and CONRAD settings at Station F.

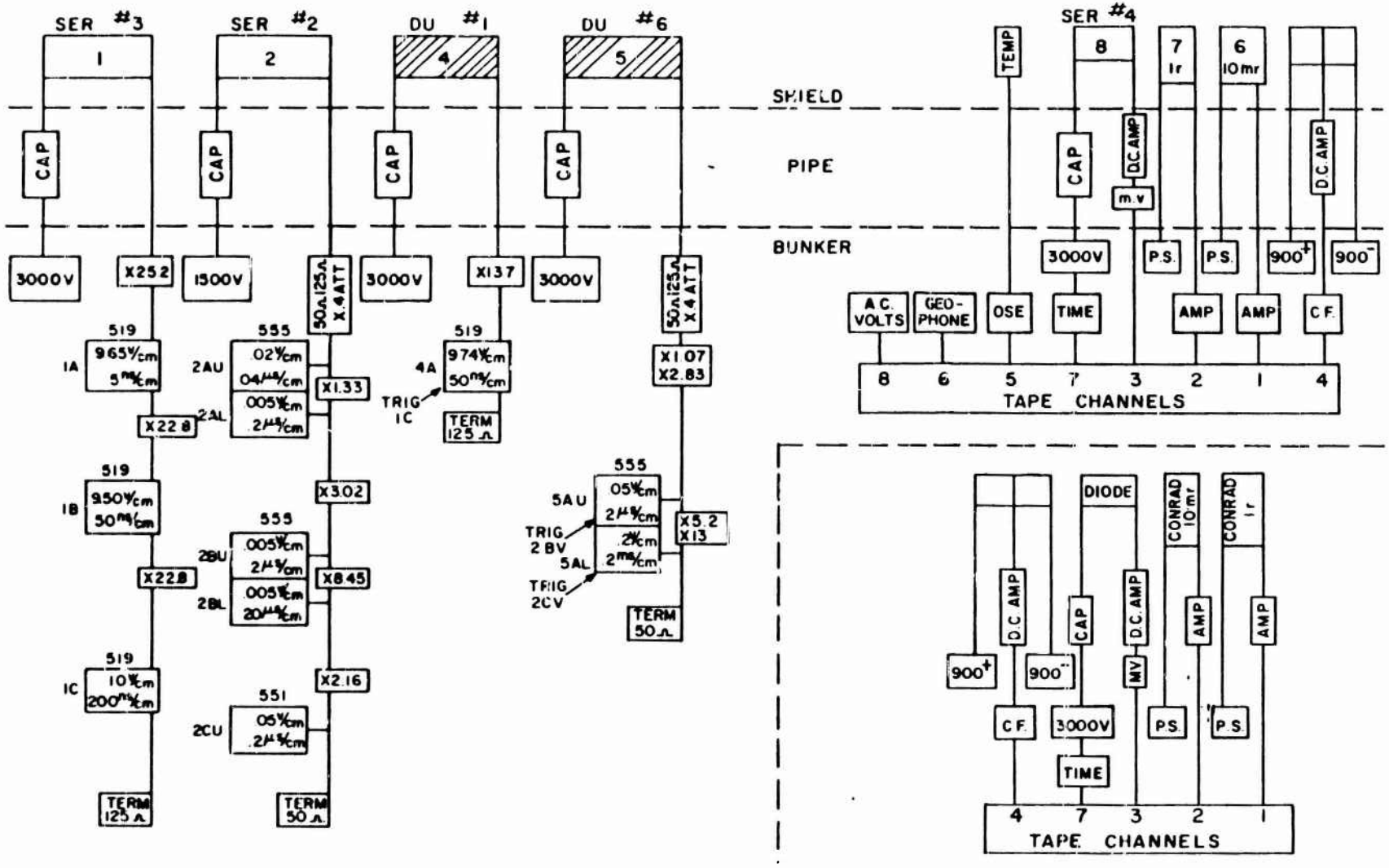

Figure 2.14 Instrument layout, oscilloscope and CONRAD settings at Station G.

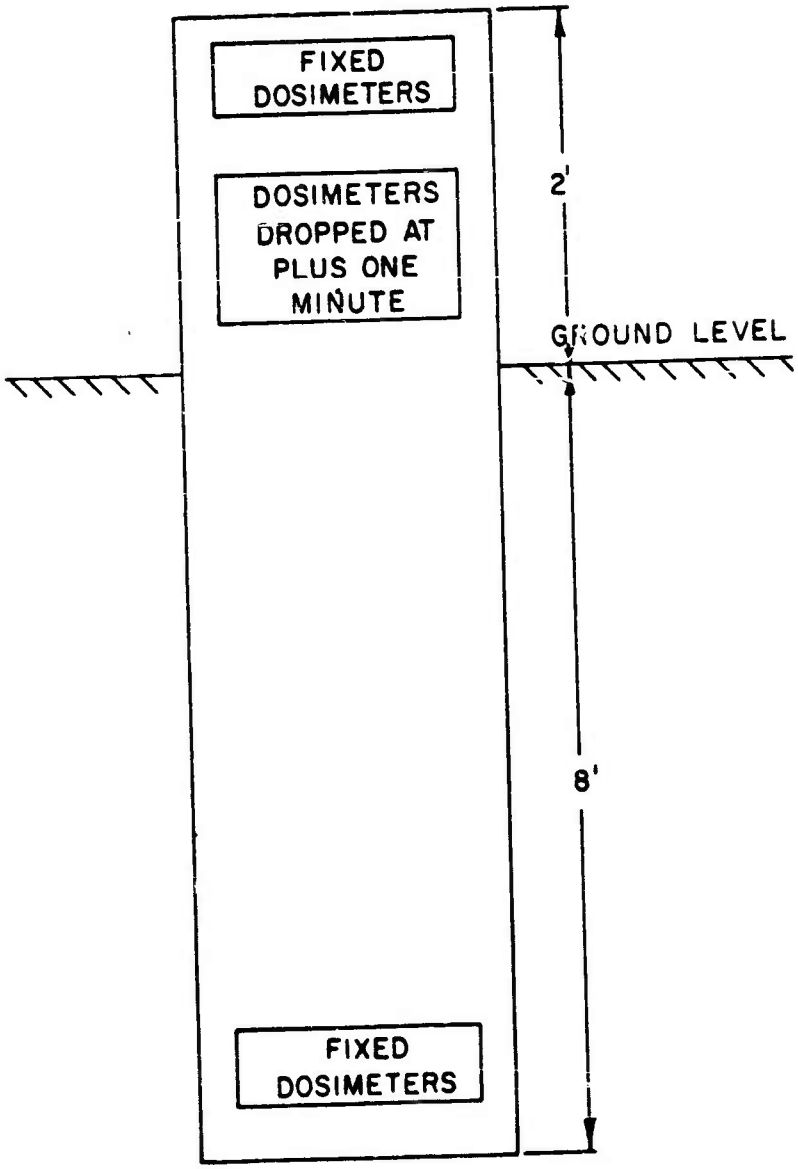

Figure 2.15 Total-dose measurement station near Station E, F, and G bunkers.

CHAPTER 3

RESULTS

3.1 DETECTOR CALIBRATION

3.1.1 Total Dose. The film portion of the total-dose gamma dosimeters was calibrated on a 100-curie Co^{60} source at NTS. Their exposure started at zero time and was completed in 20 hours, so that the latent image fading would be approximately the same as that of the film dosimeters in the field. The exposed calibration film was sent back to NDL with the recovered dosimetry to be developed simultaneously. Other total-dose gamma detectors were calibrated by NDL (Project 2.3).

3.1.2 Diode Calibration. The gamma diodes or SEMIRADS were not calibrated at NTS. They were, however, checked for adequacy of vacuum. The only way to test their vacuum was to expose them to a known gamma field and make a current-versus-voltage plot. (The signal current should level off at around 100 volts and show no change up to several thousand volts.) Leaky diodes could not be repaired and had to be replaced.

Rough handling caused cracks in some of the ceramic insulators and accounted for more damage than could be covered by spares. Fortunately, one-liter-per-second vac-ion pumps could be purchased, already evacuated and sealed, to be used as SEMIRAD gamma detectors, with only slight modification. Two of these were used in the CONRAD recording systems.

For the purposes of this report, calibration of the diodes at high intensity (SPRF and LINAC) will be used: 2.52×10^{-16} amp. The calibration of the individual diodes varies from this value by a small amount.

3.1.3 Thermistor Temperature Detector Calibration. The temperature in the detector shield of the 4,000-foot station was remotely recorded on tape, using the thermistor to vary the frequency of the blocking oscillator from the standard radiosondes. Calibration of this detector is given in Table 3.1.

3.2 AMPLIFIER CALIBRATION

3.2.1 Oscilloscope Amplifier Calibration. The amplifiers used to boost the signal for oscilloscope recording were calibrated at first using the square-wave generator of the oscilloscope output, and were photographed with the oscilloscope cameras. Last-minute changes in the input and output impedance of the amplifiers changed both their planned amplification factor and their designed clipping time. The photographs of these calibrations are not included in this report as they are known to be inadequate. The amplification factors used in this report were obtained after the shot by recording at the inputs and the outputs from a pulse generator, and by comparing the amplitudes. Because of the clipping time problems, the amplification factor as a function of frequency posed a serious problem and in many cases made the analysis of the results not reliable.

3.3 SENSITIVITY

Tables 3.2 through 3.4 list the sensitivities in r/hr/cm amplitude as well as sweep speed, for each signal trace of the oscilloscope where some data were observed. The poor design of the homemade amplifiers made them frequency dependent, and therefore the establishment of amplification factors became a difficult task.

The traces are identified in the following manner: the first number indicates the number of the detector; the second-place letter indicates the scope position in the series viewing the signal from the detector; the third position indicates the beam in the case where a two-beam scope was used; and the fourth position indicates the chopped trace, if the beam was chopped. For example, 4BUA is the trace from detector No. 4; it is the second scope in the series as indicated by the letter B; it is the upper beam as indicated by the letter U; and it is the upper trace of the chopped beam as indicated by the letter A.

3.4 DATA

3.4.1 Total-Dose Data. The total-dose data were recovered and then evaluated by NDL. The dosimeters were made up into packages of four types: Type 1 consisted of (a) an NBS holder with 649-0, 508, 510, and 1290 emulsions; (b) sulfur, gold, and cadmium-shielded gold foils; and (c) glass rods with and without lithium shields, NBS film holder inside lithium shield (emulsions as in (a)), and chemical dosimeters.

Type 2 consisted of an NBS film holder with 649-0, 508, 510, and 1290 emulsions; and sulfur, gold, and gold in cadmium shield. Type 3 consisted of an NBS film holder with 649-0, 508, 510, and 1290 emulsions. Type 4 was a low-range film dosimeter package.

A list of the total-dose dosimeters and their locations follows: At the 625-foot station: A Type 1 dosimeter package was located both inside and outside the detector shield behind the collimator; inside the uncollimated instrument shield; in the drop station; inside the CONRAD shield; and fastened to the outside of the drop station. At the 1600-foot station: A Type 1 dosimeter package was located in the instrument shield; the aluminum CONRAD shield; the steel CONRAD shield; inside the drop station; and taped to the outside of the drop station. A Type 3 dosimeter package was located at the mouth of the 8-inch cable pipe inside the bunker. A Type 4 dosimeter package was located at the center of the scope rack inside the bunker. At the 4,000-foot station: A Type 1 dosimeter package was used inside the instrument shield; inside the drop station; and was taped to the outside of the drop station. A Type 3 dosimeter package was used at the mouth of the 8-inch cable pipe inside the bunker, and a Type 4 package was used at the center of the scope rack inside the bunker.

In addition to the above dosimetry, each station was to have threshhold-type neutron detectors with a pullout.

Table 3.5 lists the total gamma and neutron doses at the points where the sensors were located. The data for neutrons were computed from the NDL evaluation of the drop-station measurement by comparing the USAELRDL sulphur measurement with the NDL measurement. Using this factor, the detailed NDL measurement was adjusted to each sensor location. The Au data shown in Table 3.5 were taken at the exact location.

The dosimetry inside the bunkers and other shielded areas showed only very low doses that could not possibly have influenced the recording of the data. These total doses are not listed in this report.

3.4.2 Gamma-Dose-Rate Data. The recovered gamma-dose-rate data recorded on magnetic tape were returned to the laboratory for reduction and analysis. Signals were found at these locations: F Bunker. F outside aluminum shield, F outside iron shield, and G Bunker. The records were transferred from tape to photographic film and then evaluated by counting the number of recorded pulses per time unit of the recording. This number is proportional to the gamma dose at the particular time. The digital readout of the CONRAD results is presented in Tables 3.6 through 3.9.

After recovery, the oscilloscope pictures were developed and shipped to USAELRDL. The oscilloscope traces were evaluated using a projector of the type Richardson Camera Co. Model VF 55M. Using this machine,data in digital form were obtained that could then be evaluated in terms of radiation intensity as a function of time.

In several cases the trace on the emulsion had to be chemically intensified. These photographs cannot be reproduced in print, and are therefore shown as drawings.

The following oscilloscope recordings provided traces that can be related with nuclear radiation: G2CU, G2BU, G2AL, GIC, GIB, F1A, F1B, F1C, E3D, E3C, E3A, E1B, and E1A. They are all shown in Figures 3.1 through 3.15. The traces E5A, E6AU, E6ALA, E7ALB, F5A, F2AU, F2AL, F2BU, F2CU, F2CL, G4A, G5AU, and G5AL were from dummies. These traces do not show signals except in the cases of traces E6AU, E6ALA, and E6ALB, where a strong signal was measured, but later it was found that this signal was from ionization because the dummy that supplied it was broken. Another dummy at F (Traces F2BU and F2BL) was interchanged erroneously with a gamma detector, and therefore its readout system was self-triggering as is evident from Figure 2.13. It did not trigger at time zero, but apparently much later, when the shock wave arrived. This indicates that no signal came from this dummy at about time zero. Therefore, it is concluded that side effects, such as cable effects, EM effect, and ionization were eliminated by proper design of the experiment and did not influence the sensor outputs.

The following is a list of traces that did not yield any results. They include pictures where the scope did not sweep; where the film exposure was so low that even the strongest chemical intensification of the negative did not bring out the trace; and where the obtained

traces had nothing whatsoever to do with radiation because of obvious electronic trouble: G2BL, G2AU, G1A, F6AU, F6ALA, F6ALB, F1D, E4DU, E4DL, E4CU, E4CL, E4BU, E4BL, E4AU, E2BL, E4AL, E2DU, E2DL, E2CU, E2CL, E2BU, E2AU, and E2AL.

Among the oscilloscope traces that did show a signal that could be correlated with gamma radiation, only those were considered in the final analysis that were reasonably free of distortion from poorly performing electronics. The correction of recordings with distortion was attempted by means of a mathematical analysis, but in most cases the distortions were too great to make possible the restoration of the original pulse. The time history of the gamma radiation for each of the three stations was reconstructed from the picture data together with the tape data. The original data from each individual station were then transferred to the other two stations using the attenuation factors between the stations to check the general validity of the measurement. The values used for the attenuation factors were supplied by Dr. John Malik of Los Alamos Scientific Laboratory and are listed here together with the values obtained from the total-dose measurements made by NDL and USAELRDL.

Folding line (with buildup): Sulphur neutrons, 200 yards; gamma rays, 350 yards.

GAMMA ATTENUATION BETWEEN STATIONS

(with buildup)

	LASL DATA		NDL and USAELRDL DATA	
	without buildup	with buildup	based on total dose	based on 0 to 30 sec dose
Between E and F	29	17.7	23.8	23.5
Between E and G	3240	1600	2210	2630
Between F and G	113	90	93	112

In order to crosscheck the data between the stations for very early times (up to and past the peak), the attenuation factors without buildup were used because at these times the build-up cannot contribute considerably to the dose rate. For later times (0 to 30 sec), the data obtained from the drop stations were used. Since the directly readout distortionless data were very meager, an attempt was made in the analysis to draw as many conclusions as possible on the pulse shape from the physics involved in the experiment. This procedure is discussed here in detail.

On Station G the only undistorted data were obtained for the following times: 0 to 2×10^{-8} seconds (Trace G2CU), 15 to 20.5 μsec (Trace G2BU), and 4.2×10^{-4} to 22 seconds (CONRAD). However, the SEMIRAD diode that delivered the signal for the pictures became gassy. This was discovered just before the evacuation time, and the only possible thing to do was to lower its voltage from 3000 to 1500 volts to prevent gas discharge. (Such a detector still has a good time resolution, and the relatively low maximum dose rate on G should

not have saturated it. Its sensitivity, however, is much higher than in the case of a good vacuum, and its value is not known.) One of the pictures obtained from this instrument is shown in Figure 3.2. The sensitivity of the detector was too high, and therefore the initial pulse produced a large undershoot in the amplifier. Another, much smaller, pulse is also seen in this picture. This pulse peaks at 19.5 μsec, which is exactly the time-of-flight of 14-Mev neutrons minus the time-of-flight of gamma rays that were produced in the iron shield of the sensor head. Its rise time gives approximately the correct weapon temperature (see Reference 7), which confirms the hypothesis that this peak is produced by the n - γ conversion of the 14-Mev neutrons and that the n - γ conversion took place in the immediate vicinity of the detector (see Reference 7). With the known total dose of 14-Mev neutrons at G from aluminum-foil data (see Table 3.5), and the measured pulse, the peak dose rate of the 14-Mev neutrons can be computed by means of the formula:

$$\text{peak 14-Mev neutron dose rate in r/hr} = \frac{\text{total dose x peak height}}{\text{time unit in hours x area}}$$

Thus the peak neutron dose rate see Reference 7) was obtained. From previous investigations, the conversion factor was obtained for the production of gamma rays by fast neutrons within an iron shield (Reference 4):

$$N_\gamma = \frac{K n \sigma_{in} I_f^o \left(e^{-n\sigma_{in}x} - e^{-\mu x} \right)}{\mu - n\sigma_{in}} \qquad (3.1)$$

Where: N_γ = the gamma dose in rads arising from inelastic scattering of neutrons

n = number of iron nuclei per cm^3 (8.31×10^{22})

σ_{in} = inelastic scattering cross section

I_f^o = incident fast neutron flux (in this case, peak flux)

K = conversion factor rads/γ photon/cm^2 ($\sim 4.6 \times 10^{-10}$)

x = wall thickness of the iron shield (1.26 cm)

μ = linear absorption coefficient for gamma radiation in iron (0.499)

For 14-Mev neutrons, the value of 4.6×10^{-24} as cross section was assumed for the total n–γ conversion (Reference 5). The value σ_{in} = 4.6 barns was not the true cross-section value, but the cross-section value (~ 0.76 barns) multiplied by the average number of gamma rays produced for each inelastic scattering of 14-Mev neutrons in iron (Reference 6). The average energy of those gammas was somewhat less than one Mev. By substituting the values in Equation 3.1 and considering that there were 1.6×10^{-8} 14-Mev neutrons per rad, the percentage of n–γ conversion in rads per rep inside the station housing was obtained. In the case of 14-Mev neutrons and a ½-inch-thick iron shield, this amounted to 2.1 percent. The peak gamma dose rate

in the 14-Mev n–γ pulse was thus obtained, yielding the value of 5.3×10^{-14} amp/r/hr as the sensitivity of the detector, as compared with 2.52×10^{-16}amp/r/hr for an instrument with a good vacuum. This value made possible the evaluation of the pictures in terms of dose rate as a function of time. The undershoot in Figure 3.2 was evaluated by putting in the input of the original, recovered, electronics pulses of known width and height, and recording the output on the original setup. The parameters of the input pulses were changed until an accurate reproduction of the undershoot in Figure 3.2 was obtained (Figure 3.16).

The known width of the laboratory-simulated input pulse and especially its height (the pulse on the left in Figure 3.16) must then resemble closely these parameters of the original input pulse. Thus, for the original pulse, the peak of 9 volts over 125-ohm resistance was obtained, which corresponds to and a width at one-tenth of the pulse height of ~ 0.12 μsec. Knowing the conversion factor in the instrument housing for the n–γ reaction from Reference 4 for Watt-spectrum neutrons (~ 0.85%), and considering the results from Project 2.2 where the fast-neutron dose rate was measured, it is apparent that the contribution of the n-γ reaction to the gamma dose rate at the time of arrival of the Watt-spectrum neutrons was much greater than all other contributions to the gamma rate. Therefore, the Watt-spectrum results obtained in Project 2.2 at Station G were multiplied by the factor 8.5×10^{-3}, and the resulting dose rate was plotted in the appropriate interval, where no recorded data would have been available otherwise. The data shown in Figure 3.17 were thus obtained.

At Station F, few acceptable data were available, and only for the time interval from 7.6×10^{-2} to 55 seconds (CONRAD) was the direct measurement of the dose rate successful. To fill in the time interval during which the neutrons arrived, the neutron data obtained in Project 2.2 were used. (as in the case of Station G). However, at Station F and also at Station E there was not a sharp separation in time between the 14-Mev and the Watt-spectrum neutrons. It was assumed that the sharp rise and peak were composed entirely of 14-Mev neutrons, and that the part past the first 5 μsec was composed of neutrons.

Figure 3.18 is an assemblage of all fragments of the curve. Recordings of the dose rate for times later than 10^{-3} seconds were obtained on this station in the bunker shield where the sensors were behind a $\frac{1}{2}$-inch steel shield and in both outside stations that were shielded by $\frac{1}{2}$-inch aluminum and $\frac{3}{8}$-inch steel (Tables 3.6 through 3.8). The analysis procedure used on Station F was also used on Station E (625 feet). Here the distortion-free recordings cover the period 9×10^{-8} to 4×10^{-7} seconds and come from oscilloscope tracings shown in Figures 3.9 and 3.10 No CONRAD measurement was obtained at this station, one recorder did not run at all, and one tape recorder broke at the very beginning of the run while the ion chambers were still saturated. Therefore, to obtain some values for these times, the measurements at Stations F and G must be considered, and the dose-rate history for 10^{-3} to 10 seconds at Station E computed from these measurements. Comparing the CONRAD results of Stations F and G, the attenuation factors between these stations roughly apply for times less than 1 second (beginning of the fireball rise). Using the appropriate values of the attenuation factors, transfer data are obtained from G to E for the times 4×10^{-4} to 3×10^{-1} seconds, and from F to E for the times 7×10^{-2} to 50 seconds. Translation of the

neutron data obtained on Project 2.2 into gamma data applies here in the same way as in the case of Station F. All the data is shown in Figure 3.19.

The collimated measurement at Station E was intended for early times only. This measurement gave very few results, and it is not possible to fill out the holes in this measurement using other recorded data. The recorded portion is shown in Figure 3.20. Only the period from 0 to 10^{-9} seconds is undistorted; the other data (3.8×10^{-8} to 5×10^{9} μsec) are probably distorted.

A more advanced mathematical analysis will be made at a later date using an analog computor on all doubtful traces that were not used in the assembly of the above data, and there is hope that some of the existing holes in the figures might be filled out eventually.

3.4.3 Additional Data. The following data were also recovered on the tapes at each station except at the bunker tape station at 625 feet and the outboard tape station at 4,000 feet.

The temperature in the detector shield at the 4,000-foot station was measured and recorded on Channel 5 of the bunker tape recorder. It was constant at $19^{\circ}C \pm 1^{\circ}$.

Channel 6 on the bunker stations recorded the shock detected by the geophone placed on the floor of the bunkers. Channel 7 on all tapes consisted of a 10-kc timing oscillator used as a time base for the tapes that provided data at Bunkers F and G. Channel 8 of all bunker tape recorders was used to monitor the ac voltage and frequency in the bunkers during the shot.

A thermograph record was made of the ambient temperature in the bunkers during the shot and is shown in Figures 3.21 through 3.23.

TABLE 3.1 TEMPERATURE DETECTOR CALIBRATION AT THE SHIELD OF STATION G

^{o}C	pulses/sec
25	54.3
30	62.5
35	72.9
40	88.4
45	102.0
50	117.9
55	133.3
60	142.8
65	154.0
70	180.0
75	188.6
80	200.0

Pages 63 through 88 deleted.

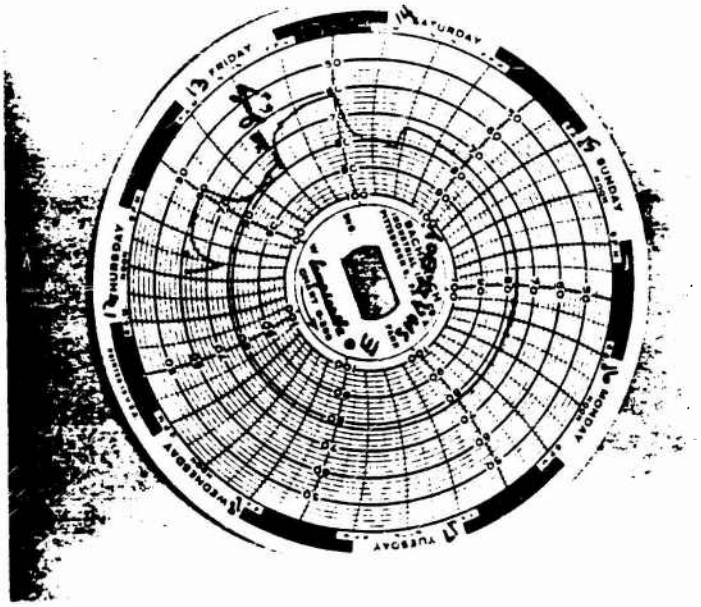

Figure 3.21 Thermograph record at the Station E bunker.

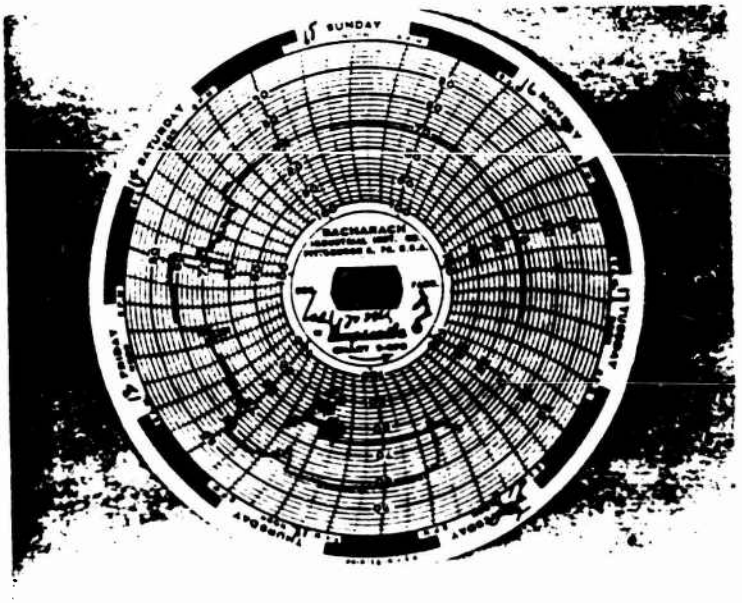

Figure 3.22 Thermograph record at the Station F bunker.

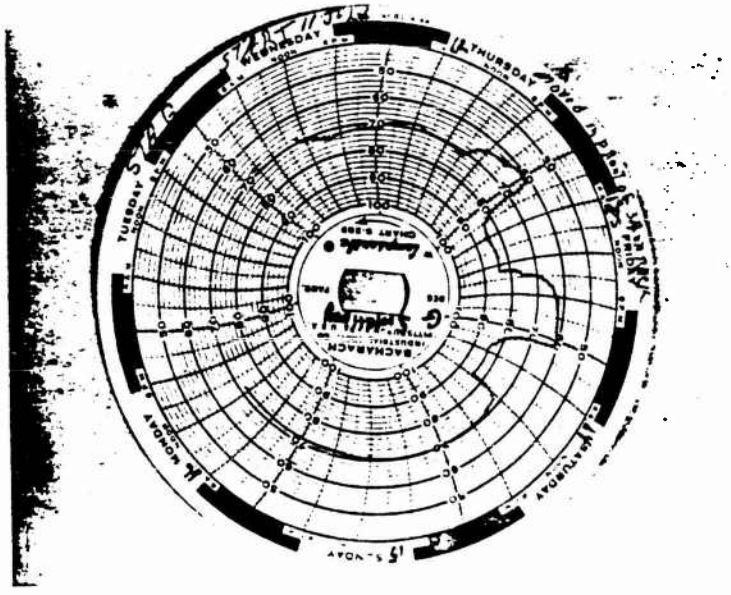

Figure 3.23 Thermograph record at the Station G bunker.

CHAPTER 4

CONCLUSIONS

The results of the measurement of the gamma dose rate as a function of time are fragmentary and represent a direct, undistorted measurement in only a few intervals. To obtain data that were usable for the correlation between the nuclear radiation and the EM effect, it was necessary to use interpolation of data among the stations and some unusual techniques of analysis as, e.g., at Station G. The overall results seem to be reasonable, and if the radiation-intensity-as-a-function-of-time data had been recorded directly at all stations and for all times, the results could not have been too different from those shown in Figures 3.17 through 3.19.

The results were very interdependent, and very few cross checks on the data were available. One cross check was the comparison of the attenuation at the peaks of the dose rates among the stations that corresponded well with the attenuation data. These attenuation factors were not used in the determination of the peaks. Another cross check was at Station F where three parallel measurements were made for the later times. The main problems encountered in the data collection came from amplifiers between the sensors and the oscilloscopes. In a few cases the failure of the detector (outgassing), a bad oscilloscope, or human factors accounted for missing data. Particular care was taken to insure that no signals other than those produced by the nuclear radiation in the sensors contributed to the results.

The possibility of distortion of the input signal by the EM effect, radiation effects in cables, ionization, or other effects that are difficult to predict was considered. Several approaches were taken to prevent these distortions or to correct for them.

The bunker stations were carefully EM- and radiation-shielded. The hollow spaces between wires in the connectors, etc., were filled with potting compound to prevent ionization, and the length of wire exposed to the direct nuclear radiation was made as short as possible. Two dummy instruments placed in the sensor heads at each bunker were used to check as to whether the different effects influenced the measurements. As described earlier the dummies did not show any output that could influence the radiation-intensity measurement. The results (Figures 3.17 through 3.20) showed the radiation intensity as a function of time for the inside of the instrument housings at each bunker. The question may arise as to what the values would have been if the detectors had not been enclosed by the ½-inch iron shield. It is believed that the results would not have differed greatly from those given in this report. The early part would have been higher by the attenuation factor in the shielding for the early gamma. The same applies for the times later than one μsec. The gamma dose rate produced by the inelastic scattering of neutrons at their arrival times would have been smaller (by a factor of ~2) than shown in Figures 3.17 through 3.19 (provided the measurements were carried out close to the ground), because the cross sections for different materials do not differ considerably at higher neutron energies.

CHAPTER 5

RECOMMENDATIONS

The data collected by Project 6.4 could be improved if a similar experiment were carried out in the future using the experience gained during Shot Small Boy. It is recommended that a future experiment should involve the following: much lighter (but tightly EM-shielded) confinement of the experimental arrangement than the presently used bunkers; improved and fast tape recorders with a time resolution of 10^{-7} seconds, instead of slow-sweep oscilloscopes; and only a few fast scopes of Type 519 for the earliest times. It is imperative either to use the highest quality electronic equipment available or to omit it. Future use of the SEMIRAD diode is recommended in all cases where the gamma intensity is very high and/or changes rapidly with time, and where the gammas arrive mixed with neutrons.

APPENDIX A

SEMIRAD THEORY

A.1 SEMIRAD SENSITIVITY

One of the unique features of SEMIRAD is the capability of varying its sensitivity over wide ranges without a change in the size of the detector (which is necessary in conventional ion-chamber detectors). The SEMIRAD system is about 10^4 times less sensitive than an ion-chamber dosimeter with a similar geometry. SEMIRAD sensitivity can be increased by the use of a large emitting surface coated with a high-yield secondary-electron emitter (for example, cesium-antimony coating as used on photomultiplier dynodes). To lower the sensitivity, a very small emitter and a low-yield emitter coating (for example, carbon) are used.

Although low-energy secondary electrons are emitted from both the positive and the negative electrodes in a SEMIRAD, the presence of the electric field causes the negatively charged electrons emitted from the positive electrode to return immediately to that electrode, and only the electrons emitted from the negative electrode traverse the detector. Thus, only the negative electrode plays an important part in SEMIRAD secondary-electron generation (in some respects, the negative electrode of a SEMIRAD is analogous to the cathode of a thermionic diode). The sensitivity of a SEMIRAD is proportional to the product of the yield and the area of the emitting (negative) surface.

If subscripts 1 and 2 denote the corresponding electrodes, the following expressions are obtained:

$$S_1 \propto A_1 Y_1 \qquad \text{(for electrode 1 as the emitter)}$$

and (A.1)

$$S_2 \propto A_2 Y_2 \qquad \text{(for electrode 2 as the emitter)}$$

Where: S = the sensitivity of the SEMIRAD (charge/rad)

A = the area of the emitting electrode

Y = the secondary-electron yield of the electrode

If both electrodes are made of material of identical composition and surfaces, then:

$$S_1/S_2 = A_1/A_2 \qquad \text{(A.2)}$$

This relation, showing that the sensitivity ratio of a SEMIRAD operated with different electrode polarities is equal to the ratio of the emitter surface areas, has been tested experimentally several times and has been found to be true provided the vacuum is good enough. This polarity dependence is one identifying characteristic of SEMIRAD operation and has been used to determine the degree of vacuum existing within SEMIRAD chambers. If, for a cylindrical SEMIRAD, S_1/S_2 is found to be closer to the value one than its computed value, and if the absolute values of S_1 and S_2 begin to increase, the vacuum is probably

poor, and ionization is taking place within the detector.

A.2 SEMIRAD VACUUM CONSIDERATIONS

The vacuum in SEMIRAD serves two purposes: (1) it eliminates gas ionization, and (2) it makes possible the collection of low-energy secondary electrons. SEMIRAD vacuum requirements can be determined by considering these two purposes. If the arbitrary (but reasonable) ion-production limit of one ion pair for every 50 secondary electrons is chosen, then the ionization response of SEMIRAD is no greater than two percent of the total response. To achieve this goal, the gas pressure within the detecting chamber must be reduced until the sum of the production of ions by both primary radiation and ion multiplication is less than two percent of the number of secondary electrons produced.

The number of ions produced within an ion chamber by primary particles emerging from the wall of the chamber may be calculated from the following easily derived relation that assumes linear energy transfer of the primary particles:

$$N = E_p Pd/760WR \qquad (A.3)$$

Where: N = the number of ions formed per primary particle

E_p = the energy of the primary particles (ev)

P = the gas pressure within the ion chamber (mm Hg)

d = the mean free path of the primary particle within the chamber (cm)

W = the average energy required for the production of one ion

R = the range of the primary particles in the gas at normal pressure (cm)

If this relation is used and the yield of the SEMIRAD surface (the number of secondary electrons emitted for each primary particle) is taken into account, the pressure required is as follows:

$$P \leq 760\ WRN\ y/E_p d \qquad (A.4)$$

Where: y = the yield of the SEMIRAD surface (electrons/primary particle)

Considering a 1-Mev electron whose range is 400 cm in air, and using W = 32.5, N = 2/100, y = 2, $E_p = 10^6$ ev, and d = 2 cm, the necessary air pressure is found to be 0.2 mm Hg.

In order to limit the production of gas ions by the passage of accelerated secondary electrons through the chamber to less than two percent of the total response, the residual gas pressure must be limited so that the probability of an individual secondary electron causing the formation of an ion pair during its chamber transit is less than 2/100. This is done by adjusting the residual gas pressure within the SEMIRAD until the mean free path of the electrons becomes 50 times the collection distance.

Since the mean free path of an electron in air can be expressed by $L_e = 4.1 \times 10^{-2}/p$, where L_e = the mean free path of the electron (cm), the pressure becomes:

$$P \leq 4.1 \times 10^{2}/50d$$

For d = 2 cm, the pressure required is 4.1×10^{-4} mm Hg or less. Since this pressure is less than that previously calculated, it sets the vacuum requirements for SEMIRAD operation.

A.3 SEMIRAD DOSE-RATE LIMITATIONS

Since SEMIRAD are electronic diodes in which the electrons are generated by high-energy radiation rather than by thermionic emission, the current limitations for thermionic diodes apply also to SEMIRAD. These limitations are the result of space-charge formation between the emitter and the collector, and are given in Reference 2. In this paper, Langmuir and Compton compute limits for several geometrical arrangements of the emitting and collecting electrodes. The results applicable to SEMIRAD are given below and are based on the assumption that the electrons are emitted with negligible initial velocities.

For coaxial cylinder geometry, as used on Shot Small Boy, the expression for the limiting current in a SEMIRAD depends on which electrode is the emitter, and on the relative radii of the electrodes. The limiting current for both cases is given by the following parametric equation:

$$i = \frac{2}{9}(2e/m)^{\frac{1}{2}}(LV^{3/2}/r\beta^2) \quad \text{or} \quad i = 14.68 \cdot 10^{-6}\, LV^{3/2}/r\beta^2 \tag{A.5}$$

Where: r = the collector radius (cm)

L = the length of the cylinder (cm) ($L \gg r$ for negligible end-effect correction)

β = a parameter depending on the geometry used

If r_e is the emitter radius, then for $r_e/r < 1$ (external collector):

$$\beta = 1 + 0.9769\,(r_e/r)^{2/3} \sin\left[1.0854\,\{\log(r/r_e) - 1.0766\}\right] \tag{A.6}$$

If $r_e/r > 1$ (internal collector), then:

$$\beta^2 = 4.6712\,(r_e/r)\left[\log(r_e/r) - 0.15045\right]^{3/2} \tag{A.7}$$

A.4 SEMIRAD ENERGY DEPENDENCE

Energy dependence of a radiation-measuring system is defined as the variation of the system response to a given constant quantity of incident radiation as a function of the quantum energy of the incident radiation. This definition indicates that any statement on energy dependence of an instrument depends on the units in which the quantity of the incident radiation is measured.

The quantity of radiation can be expressed in: (a) the number of particles incident on a unit area at the point of the measurement: (b) the total energy (in ergs) that passes a unit area at the point

of measurement; (c) the energy delivered by the incident radiation to a sample of a certain material with a given volume or mass; or (d) the number of ion pairs that can be produced by radiation in a given volume of gas. In the study of radiation effects, the energy absorbed in the irradiated sample is in most cases the important factor, and therefore many investigators use the rad as a unit of measurement. By definition, one rad is delivered when a given sample of one gram mass absorbs 100 ergs of energy. This unit is dependent on the irradiated material, and therefore the terms aluminum rads, tissue rads, etc., are used.

A.5 SEMIRAD ENERGY DEPENDENCE FOR GAMMA RADIATION

Suppose a gamma-sensitive SEMIRAD is irradiated with gamma rays that have the spectral distribution $\frac{dI}{dE}$ (E), where I is the intensity measured in rads. These gamma rays cannot directly transmit their energy to the wall of the instrument, but they will produce high-energy electrons by means of photo effect, Compton effect, and pair production. On the first-collision basis, these electrons will be, according to their energy, in equilibrium within the cavity of the SEMIRAD. This is true provided that the distance between the border surface of the cavity and the outside wall is much smaller than the mean-free path of the lowest-energy gamma and bigger than the maximum range of the highest-energy electron that can be produced by gamma spectrum.

An electron spectrum that can be experimentally measured inside the SEMIRAD cavity can be expressed as follows:

$$\frac{dI_e}{dE}(E) = F\left[\frac{dI_\gamma}{dE}(E)\right] \qquad (A.8)$$

(F contains the wall material as a parameter)

By choosing a very thin layer of material adjacent to the cavity wall with the thickness Δx, where Δx is much smaller than the effective electron range, it is found that the energy deposited in this thin layer by the electrons or indirectly by the gamma rays (which is the energy delivered to the volume $A\Delta x$, where A is the cavity area) is as follows (in rads):

$$D = \int_E^\infty \frac{dI_e}{dE}(E)\ \frac{dE_e}{dx}(E) A\Delta x 2\, dE \qquad (A.9)$$

$\frac{dE_e}{dx}(E)$ is the energy loss of the fast electron per unit distance traveled in the wall material. This loss is a function of the electron energy, but can be assumed to be constant in the thin layer Δx, because the change of electron energy caused by this layer is small. Factor 2 in A.9 indicates that every electron that traverses the vacuum has to cross Δx twice.

The charge that flows through the collecting electrodes of the SEMIRAD is then computed. If $Y_i(E)$ is the isotropic yield for production of low-energy secondary electrons by the fast primary electrons with energy E, then the total charge released from the wall in the form of

secondary electrons with the spectral distribution $\frac{dI_e}{dE}$ (E) will be

$$Q = \int_{E=0}^{\infty} \frac{dI_e}{dE} (E)\ Y_i\ (E)\ 2\ e\ A\ dE, \qquad (A.10)$$

where e is the electron charge. It can be shown that Y_i (E) = 2Y(E), where Y(E) is the yield for perpendicular incidence, and according to calculations and measurements, Y(E) is proportional to the energy delivered by the primaries to a thin surface layer of the target from which the secondary electrons can emerge:

$$Y_i\ (E) = K \frac{dE_e}{dx} (E)\ \Delta S \qquad (A.11)$$

Where: K = a proportionality factor

ΔS = the thickness of the escape layer

Substitution of A.11 into A.10 yields:

$$Q = \int_{E=0}^{\infty} \frac{dI_e}{dE} (E)\ K \frac{dE_e}{dx} (E)\ \Delta S\ 2\ e\ A\ dE \qquad (A.12)$$

Setting $\Delta S = \Delta x$ and considering A.9, one obtains:

$$Q = EKD \qquad (A.13)$$

This means that the charge collected in a SEMIRAD which was exposed to a certain gamma-ray dose measured in rads is proportional to this

dose, regardless of the energy of the incident gamma rays, provided the restrictions under which this expression was derived are observed. In addition to the restrictions mentioned before, this statement applies only to SEMIRAD with 4π geometry, which is approximately true in the case of the instruments constructed for Project 6.4.

REFERENCES

1. G. Carp and others; "Initial-Gamma Radiation Intensity and Neutron-Induced Gamma Radiation of NTS Soil (U)"; Project 2.5 Operation Plumbbob, WT-1414, April 1961: U.S. Army Signal Research and Development Laboratory, Fort Monmouth, New Jersey; Secret Restricted Data.

2. I. Langmuir and K.T. Compton; Rev. Mod. Phys. 3, 2, p. 191, April 1931.

3. "Small Boy Pretest Analysis (U)"; Planning Report No. 1; 6 April 1962; Research Directorate, Air Force Special Weapons Center, Kirtland Air Force Base, New Mexico; Secret Restricted Data.

4. R. Smith and R. Benck; NDL-TR19, November 1961; Nuclear Defense Laboratory, Edgewood Arsenal, Maryland.

5. V.E. Scherrer, R. B. Theus, and W. R. Faust; Phys. Rev. 89, 1268, 1953.

6. I. Troubetzkoy and others; NDA 211-3, Vol. C, P. 10, 1 November 1959; Nuclear Defense Agency, Aberdeen, Maryland.

7. S. Kronenberg, B. Markow and I.A. Balton; "Measurement of Fast Neutron Dose Rate as a Function of Time (U)"; Project 2.2, Operation Sun Beam, Shot Small Boy, POR-2210; U.S. Army Electronics Research and Development Laboratory, Fort Monmouth, New Jersey; Secret Restricted Data.

Page 105 deleted.